https://ntrs.nasa.gov/search.jsp?R=19690021954 2020-03-12T03:37:07+00:00Z

General Disclaimer

One or more of the Following Statements may affect this Document

- This document has been reproduced from the best copy furnished by the organizational source. It is being released in the interest of making available as much information as possible.

- This document may contain data, which exceeds the sheet parameters. It was furnished in this condition by the organizational source and is the best copy available.

- This document may contain tone-on-tone or color graphs, charts and/or pictures, which have been reproduced in black and white.

- This document is paginated as submitted by the original source.

- Portions of this document are not fully legible due to the historical nature of some of the material. However, it is the best reproduction available from the original submission.

Produced by the NASA Center for Aerospace Information (CASI)

RYAN

FACILITY FORM 602

N69-31332

(ACCESSION NUMBER) 95 (PAGES)

NASA CR-101776 (NASA CR OR TMX OR AD NUMBER)

(THRU) 1 (CODE)

14 (CATEGORY)

NASA CR 101776

REPORT NO. 57667-4

SCATTEROMETER DATA ANALYSIS PROGRAM

FINAL REPORT

For the Period June 1, 1968 to May 31, 1969

PREPARED BY: N. Guillot and S. Benedict

PREPARED FOR: NASA MANNED SPACECRAFT CENTER
HOUSTON, TEXAS
UNDER CONTRACT NO. NAS 9-8252

PREPARED BY: RYAN AERONAUTICAL COMPANY
5650 KEARNY MESA ROAD
SAN DIEGO, CALIFORNIA 92112

TABLE OF CONTENTS

SECTION	TITLE	PAGE
1	INTRODUCTION	1-1
1.1	PROGRAM OBJECTIVES	1-1
1.2	BACKGROUND	1-2
1.3	RECOMMENDATIONS	1-3
2	DATA REDUCED AND EVALUATED	2-1
2.1	MISSION 61, SITE 76, FLIGHT 3, RUN 1, LINES 1-5 AND FLIGHT 4, RUN 1, LINES 1 AND 2	2-1
2.2	MISSION 70, FLIGHTS 2, 3, AND 4	2-4
2.3	MISSION 72, SIGHT 167, FLIGHT 3, LINE 1, RUN 2A; LINE 1, RUN 2B AND LINE 2, RUN 1	2-9
2.4	MISSION 73, FLIGHT 1, SITE 130 LINES 8 , 9, 10, 11, 12, AND 15	2-9
2.5	MISSION 74, FLIGHTS 1, 2, AND 4	2-11
2.5.1	Flight 1, Site 76	2-12
2.5.2	Flights 2 and 4	2-12
2.6	MISSION 75, FLIGHT 3, RUN 1 OF LINES 10, 11, 12	2-12
2.7	MISSION 76 (25 LINES)	2-12
2.8	MISSION 77, SITE 44, FLIGHT 2, LINE 31, RUN 1	2-15
2.9	MISSION 80	2-17
2.10	MISSION 81, SITE 132, FLIGHT 9, LINE 1, RUN 1	2-18
2.11	MISSION 88, SITE 184	2-20
3	PROGRAM CAPABILITIES	3-1

TABLE OF CONTENTS

SECTION	TITLE	PAGE
3.1	OUTPUT FLEXIBILITY OF BASIC 13.3 GHz PROGRAM	3-1
3.2	DISCUSSION OF 1.6 GHz AND 400 MHz PROGRAM REQUIREMENTS	3-2
3.3	GENERAL DISCUSSION OF BASIC 13.3 GHz PROGRAM	3-4
4	SCATTEROMETER DATA DISPLAY USING THE SPATIALLY ADJUSTED TIME HISTORY PLOT . . .	4-1
5	DATA VALIDATION	5-1
5.1	13.3 GHz SCATTEROMETER SYSTEM	5-2
5.2	PRE-MISSION CHECK PROCEDURES	5-4
5.3	POST-MISSION VERIFICATION PROCEDURES . . .	5-7
5.4	GENERATION OF DIGITAL PSD's	5-11
5.5	DYNAMIC RANGE	5-13
5.6	TIME HISTORIES	5-14
5.7	PEAK CALIBRATE LEVEL TO NOISE MEASUREMENT	5-15
5.8	CONCLUSIONS	5-15

APPENDIXES

A	DERIVATION OF SIGN SENSING ROUTINE	A-1
B	DATA VALIDATION PROGRAM	B-1
C	CHARACTERISTIC PROBLEMS IDENTIFIED THROUGH DATA VALIDATION PROCEDURES	C-1

LIST OF ILLUSTRATIONS

FIGURE NO.	TITLE	PAGE
2-1	Mission 70, Flight 2, Hand Calculated Data . . .	2-5
2-2	Mission 70, Flight 3, Computer Calculated Data	2-5
2-3	Mission 70, Flight 4, Computer Processed Data	2-7
2-4	Comparison of Crosswind Data	2-7
2-5	Comparison of Upwind-Downwind Data	2-8
2-6	Comparison of Data Upwind-Downwind vs Crosswind	2-8
2-7	Comparison of Data	2-10
2-8	Comparison of Mission 76 Data and Mission 39 Data	2-14
2-9	Scatterometer Data With Effects of a Data Reduction Anomalie	2-19
4-1	SATH Plot Data Averaged Every 1.0 Second	4-3
4-2	SATH Plot With 0.1 Second Sampling	4-4
4-3	Data Collected at 3 Angles and Spatially Adjusted	4-6
4-4	Segment of Data From Mission 76	4-8
5-1	REDOP Block Diagram	5-3
5-2	Tape Loop Data Analysis Technique	5-5
5-3	Typical Overland Frequency Spectrum	5-5
5-4	Time History Data Analysis Technique	5-5

LIST OF TABLES

TABLE NO.	TITLE	PAGE
2-1	LIST OF EVALUATED LINES & RUNS	2-1
2-2	AREAS OF TAPE RECORDER SATURATION DUE TO COLLECTION OF OVERWATER DATA WITH OVERLAND GAIN SETTINGS	2-16
2-3	MISSION DATA REDUCTION/SCATTEROMETER STATUS AS OF 5-1-69	2-22
5-1	PROBLEMS IDENTIFIED IN THE PAST	5-8

SECTION 1

INTRODUCTION

The objective of the NASA Earth Resources Survey Program (ERSP) is to determine what contributions can be made by remote sensors to various disciplines: agriculture, forestry, geology, oceanography, weather prediction, urban programs, and others. To further these objectives the ERSP has initially adapted remote sensing technology and instrumentation, some originally developed for space application to earth resources surveying. To achieve these objectives advanced sensors and technology are being developed which will uniquely define specific earth resources from airborne and spaceborne platforms. Remote sensing surveys made from such platforms will permit synoptic measurements for directly mapping earth resources and for viewing atmospheric phenomena on a global basis.

1.1 PROGRAM OBJECTIVES

The data analysis contract (NAS9-8252) performed by Ryan Aeronautical Company is an integral part of the ERSP. The objectives of this contractual effort apply specifically to scatterometer systems. They are:

- To determine Scatterometer signatures
- To develop a library of curves of RF backscattering coefficients.
- To determine criteria for identifying surface parameters.
- To determine an economical method for reducing sea state data.
- To determine optimum data reduction methods and the most useful formats for data presentation.
- To correlate data between the 400 MHz and 13.3 GHz scatterometers.
- To determine the effects of polarization at 400 MHz.

- To determine the feasibility of terrain identification using radar signatures.
- To develop methods of determining the direction of polarization rotation.
- To determine autocorrelation functions for the 400 MHz and 13.3 GHz scatterometers.
- To analyze various surface features and types as a function of the RF backscattering coefficient.

This report summarizes the achievemensts made by Ryan on this program in fulfilling the above mentioned objectives. During this period, approximately 46 lines of scatterometer data have been processed and verified. A listing of these is provided in Section 2 of this report.

During the contract period, NASA procured two additional scatterometer systems from Ryan for their Earth Resources Survey Program. They were 1.6 GHz and 13.3 GHz dual polarized scatterometers. The 1.6 GHz scatterometer was flown on the North Atlantic Mission in March 1969. As part of this contract, Ryan has supported NASA in the validation of the data taken prior to functional check flight (FCF), and during this mission. The 13.3 GHz dual scatterometer has not yet flown.

1.2 BACKGROUND

Ryan initially designed, built, and tested a radar reflectivity system in 1962. A single polarized (REDOP) scatterometer which evolved from this prototype system was sold to NASA/MSC and installed on the CV240 in 1965. This system was built for the primary purpose of obtaining reflectivity data for evaluating the capability of doppler velocity sensors, radar altimeters, and surveillance radars. The high priority of the Apollo Program with its planned radar-directed lunar descent caused a focusing of attention on the REDOP scatterometer, as a device for obtaining backscattering data from lunar-like terrain. This data could be used specifically for

evaluating the capability of the lunar-landing radar. Though considerable data was taken with the REDOP scatterometer over various terrains, the majority of the data during 1966 and 1967 was taken over terrain which was considered analogous to the lunar surface. This program since 1967 has increased in scope and prominence to include a family of remote sensors for the purpose of surveying the surface of the earth and to the ultimate benefit of mankind by contributing valuable information for better management of our earth resources. As the scope of this program expanded so did the value of the REDOP scatterometer to the point that today four scatterometer systems are included within the family of remote sensors: 1) The original single polarized 13.3 GHz scatterometer; 2) a dual polarized 13.3 GHz scatterometer; 3) a dual polarized 1.6 GHz scatterometer, and 4) a 400 MHz scatterometer system.

As the number of scatterometers increased so did the data reduction load. The original data reduction programs were inadequate to meet the demands of this increase and are subsequently being revised.

For the past year the emphasis of Ryan Engineers has been focused primarily in three areas: 1) to develop methods of display of scatterometer data for making this data of more value to principal investigator and to the scientific community in general; 2) to validate in general, the output of the data processing programs and to check the validity of the algorithms as programmed in the digital computer programs; 3) to decrease the turn-around time of data processing by optimizing the formation of the programs. These primary efforts are discussed in this final report.

1.3 RECOMMENDATIONS

During this past year much has been learned by NASA and Ryan engineers concerning scatterometer data processing. With the increase in the number of scatterometers being flown, and the amount of data that will be handled this coming year, several potential problem areas have become apparent. In order to locate, define, and solve these problems, so that scatterometer data will flow smoothly and efficiently, the following recommendations are submitted:

- Error Analysis - A complete error analysis of each scatterometer should be made, accounting for all the electronics and perturbative effects due to specific environmental conditions.

- Scatterometer Calibration Procedures - A set of calibration procedures for each scatterometer should be defined and documented. The procedures should include pre-mission check out of equipment, functional check flight definition, and ground calibration requirements.

- Automatic Editing - The automatic editing procedures should be updated to include data from all scatterometer systems. with the increase in data due to the addition of the 1.6 GHz and 13.3 GHz dual polarized systems, automatic editing is almost imperative.

- Data Display - Effort should be continued to develop new and better data display techniques. Methods should be studied of how the data from each scatterometer can be displayed in such a way that would enhance its usefulness to NASA and the scientific community.

In addition to the above listed areas, it can be anticipated that problems normally associated with the development of new remote sensing instrumentation will periodically occur. Problems such as modifying computer programs will always be part of the data reduction program. It is felt that, with the past years of experience in the Earth Resources Survey Program, both Ryan and NASA can, as they have in the past, solve these problems as they occur.

SECTION 2

DATA REDUCED AND EVALUATED

This section lists all the lines and runs which have been reduced, evaluated, and released through NASA/MSC to Earth Resources Principal Investigators (Table 2-1). Also included are descriptions of each mission and some examples of the data.

2.1 MISSION 61, SITE 76, FLIGHT 3, RUN 1, LINES 1-5 AND FLIGHT 4, RUN 1, LINES 1 AND 2.

Mission 61 was flown in November of 1967. The data collected over Garden City, Kansas (Site 76) was in support of studies being conducted at the Unviersity of Kansas (D.S. Simonett Principal Investigator). Of primary interest was an attempt to use the 13.3 GHz Scatterometer to qualitatively describe terrain conditions, both vegetation and soil.

It was requested that "raw" filtered information from these lines be displayed in a time history format of relative voltage versus time. When this was completed the data were checked for variation in level with change in incidence angle and for stability of calibrate level. The time histories were released with two short time segments noted where the data could not be validated due to apparent noise spikes.

TABLE 2-1 LIST OF EVALUATED LINES & RUNS

Mission	Site	Flight	Line	Run
61	76	3	1	1
61	76	3	2	1
61	76	3	3	1
61	76	3	4	1

TABLE 2-1 (Continued)

Mission	Site	Flight	Line	Run
61	76	3	5	1
61	76	4	1	1
61	76	4	2	1
70	166	2	1	1
70	166	2	2	1
70	166	2	3	1
70	166	2	4	1
70	166	3	10	1
70	166	3	11	1
70	166	3	12	1
70	166	3	13	1
70	166	3	21	1
70	166	4	22	1
70	166	4	23	1
70	166	4	24	1
72	167	3	1	2A
72	167	3	1	2B
72	167	3	2	1
73	130	1	8	1
			9	1
			10	1
			11	1
			12	1
			15	1
74	85	2	3	1
74	44	4	22	1
			26	1
			27	1
74	76	1	1	1A
74	76	1	1	1B
74	76	1	3	1
75	32	3	10	1

TABLE 2-1 (Continued)

Mission	Site	Flight	Line	Run
75	32	3	11	1
75	32	3	12	1
76	56	4	1	1
			1	2
			1	3
			1	4
			1	5
			1	6
			2	1
			2	2
			2	3
			2	4
			2	5
			2	6
			2	7
76	56	5	1	1
76	56	5	1	2
76	56	5	1	3
76	56	5	1	4
76	56	5	1	5
76	56	5	2	1
76	56	5	2	2
76	56	5	2	3
76	56	5	2	4
76	56	5	2	5
76	56	5	2	6
77	44	2	31	1
80	76	7	3	1
81	132	9	1	1

2.2 MISSION 70, FLIGHTS 2, 3, AND 4

Mission 70 was flown as part of the Earth Resources Aircraft Program under the direction of NASA/MSC Science and Applications Directorate. The primary objective of the mission was to obtain overwater remote sensor information under sea state conditions in excess of 15 feet. The mission was based at Keflavik, Iceland, and the data was gathered over the North Atlantic, during April 1968. Information collected on this mission was in support of studies being carried on at the Universities of New York and Kansas. A summary of flights 2, 3, and 4 follows.

Figure 2-1 shows representative curves from four lines of flight 2. This data was gathered over 26-foot waves. One channel of the scatterometer was inoperative during this flight so that data was obtained on just one magnetic tape channel. As a result, the information could not be sign sensed or computer processed. The curves presented here were hand calculated from composite power spectral density plots. Their tendency to flatten out with a limited dynamic range is a characteristic of data from a rough surface.

A weather ship in the vicinity of flight 3 reported 19 foot waves. Since both channels were operative on this flight the representative curves in Figure 2-2 have been computer processed. The increase in dynamic range caused by a higher return from angles near the vertical and a lower return from the larger incidence angles shows the characteristics of somewhat smoother sea conditions.

It should be noted, that the level of the σ_o curves, particularly at the higher incidence angles, is known to be velocity dependent. Without accurate guidance and navigation data to update the reduction process, certain variations in the higher incidence angles can be expected.

An example of such a variation was noted during data verification of line 10, run 1 (Figure 2-2). Prior to transcription of the tape recorder voice track where more than one velocity reading could be identified, the curve had been

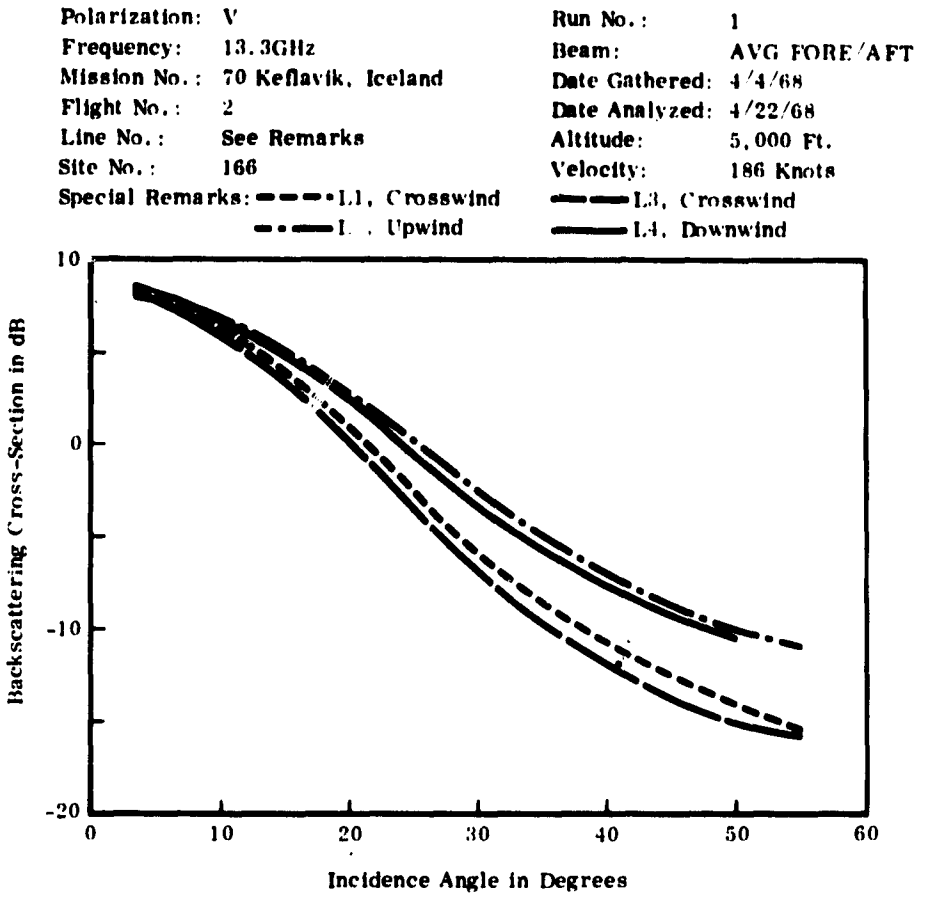

Figure 2-1 Mission 70, Flight 2, Hand Calculated Data

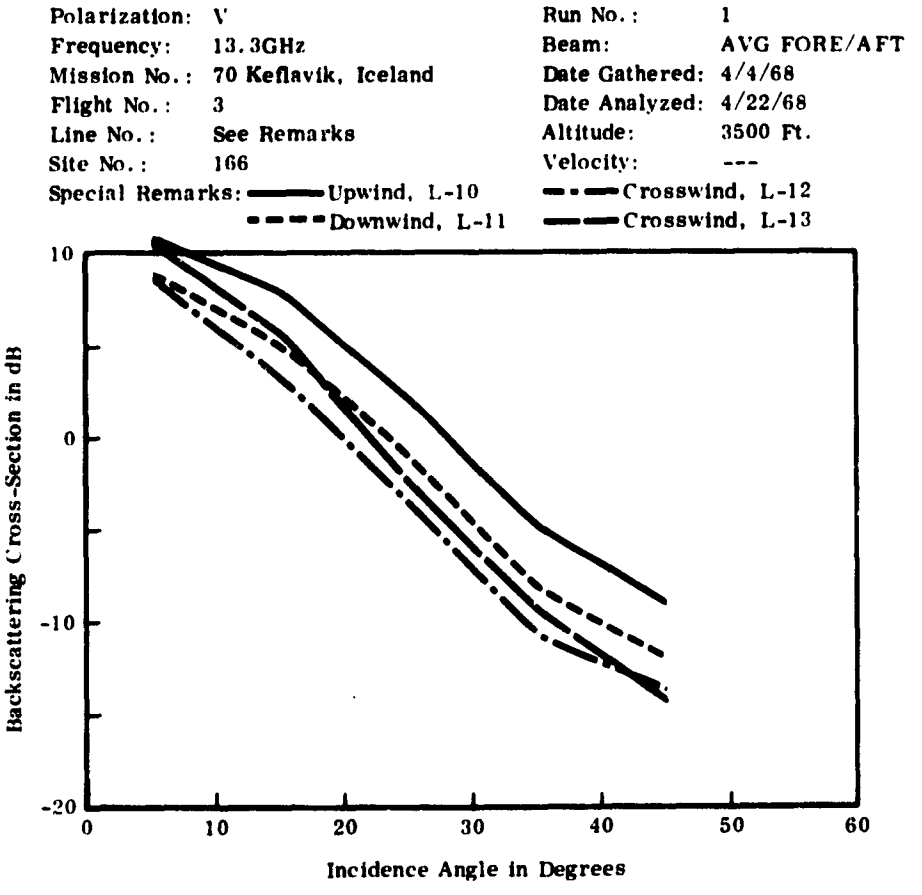

Figure 2-2 Mission 70, Flight 3, Computer Calculated Data

processed using a single velocity reading from the flight logs. The difference in σ_o at 45° incidence angle was 9 db with lesser differences noted at the lower angles.

Until an accurate update for guidance and navigation parameters is available such level variations will occur particularly on missions flown with the NASA P-3A aircraft.

Flight 4 continues the trend that the computer processed curves in Figure 2-3 show. The sea state during this flight was placed at sea state 5 with nine foot waves. The curve shapes express this change in sea state by increasing in dynamic range.

Figure 2-4 shows how crosswind curves from the three flights compare. Figure 2-5 is a comparison of their upwind-downwind curves. Noting the lack of accurate guidance and navigation parameters mentioned earlier, the curve in Figure 2-5 representing flight 3, 19-foot data does not include line 10, run 1 upwind information. This data, due primarily to poor velocity inputs, tended to pull the upwind-downwind average curve up in a region where it could not be justified. Therefore, the 19-foot wave curve presented in Figure 2-5 is only representative of line 11, run 1 downwind information.

The two sets of curves in Figures 2-4 and 2-5 then show the 13.3 GHz scatterometer's ability to detect variations in sea surface conditions.

Also of interest are the comparisons which can be made between the lines within each flight. Figure 2-6 shows the crosswind data for the 26 foot waves below the upwind-downwind data. These data correlate well with past information (Mission 60 Argentia) and with scattering theory. For the lower sea state conditions this difference is not as apparent, agreeing again with past data such as Mission 20 where wave heights were 7 feet.

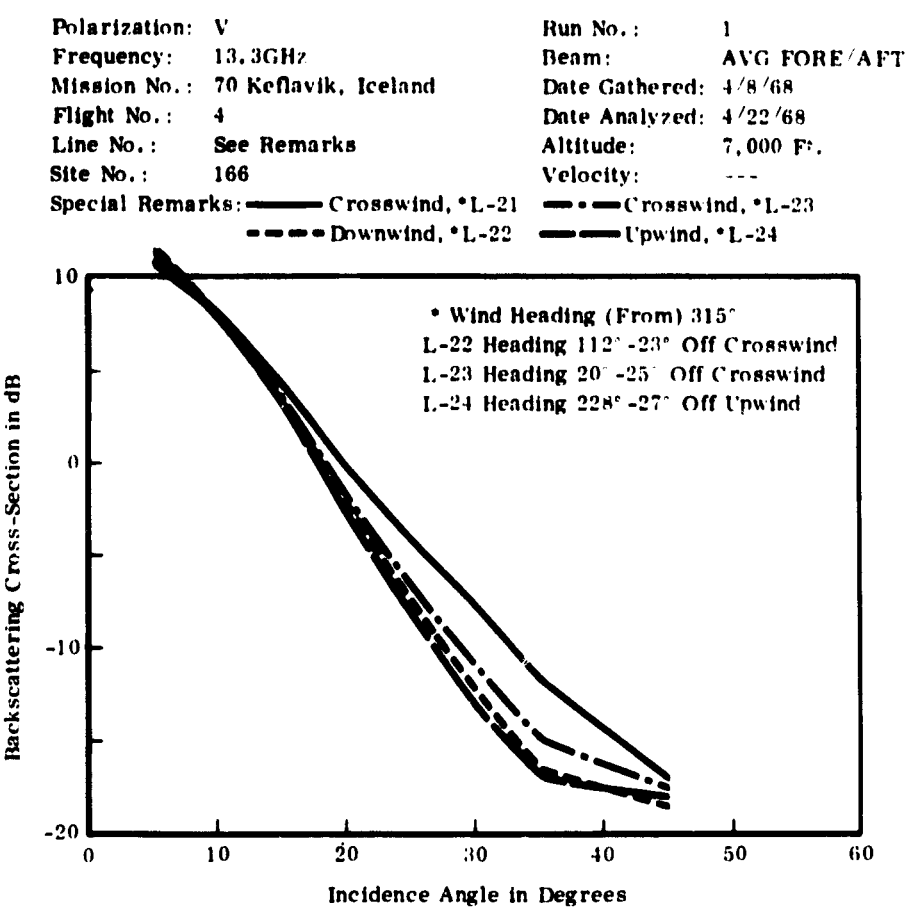

Figure 2-3 Mission 70, Flight 4, Computer Processed Data

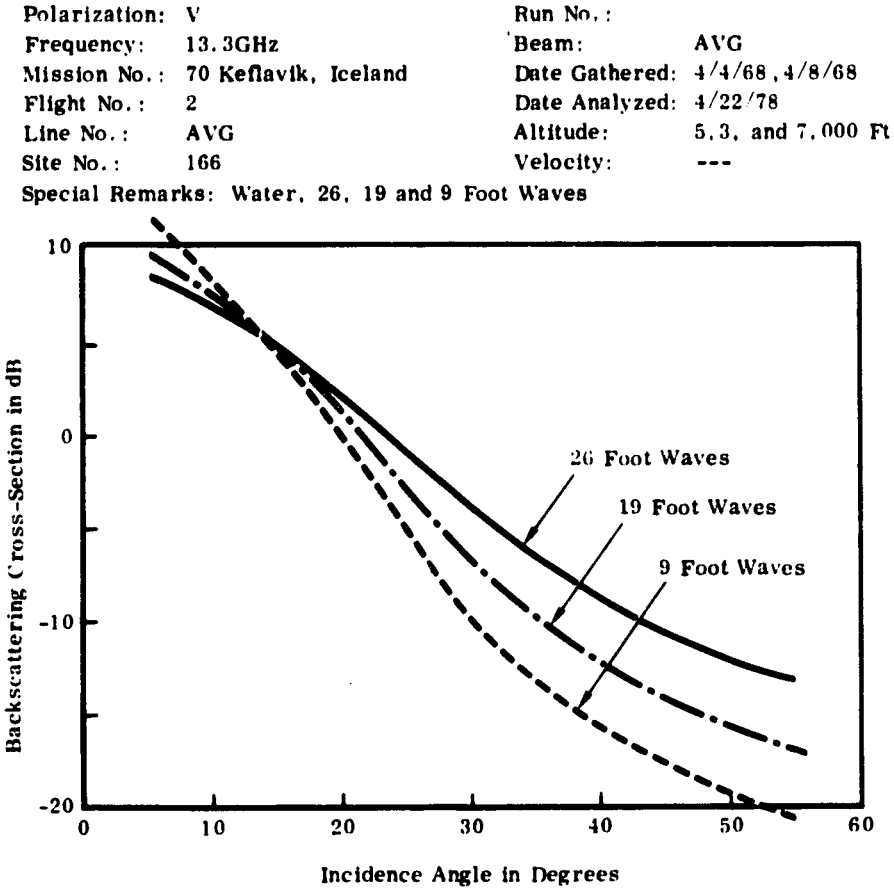

Figure 2-4 Comparison of Crosswind Data

Polarization:	V	Run No.:	
Frequency:	13.3GHz	Beam:	AVG
Mission No.:	70 Keflavik, Iceland	Data Gathered:	4/4/68
Flight No.:	2, 3, 4		4/8/68
Line No.:	Average	Data Analyzed:	4/22/68
Site No.:	166	Altitude:	5, 3 and 7000 Ft.
Special Remarks:	Water, 26, 19 and 9 Foot Waves	Velocity:	---

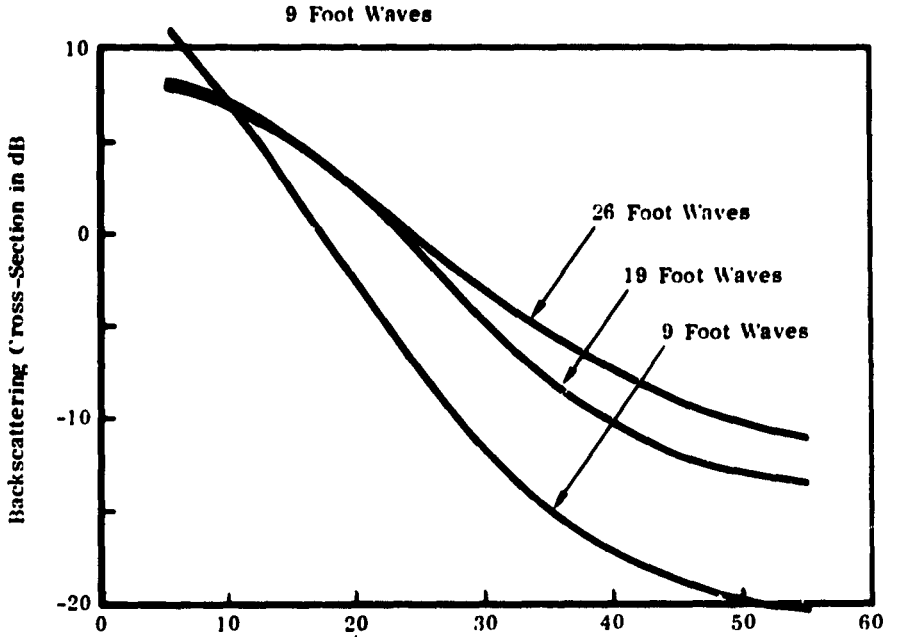

Figure 2-5 Comparison of Upwind-Downwind Data

Polarization:	V	Run No:	
Frequency:	13.3GHz	Beam:	AVG
Mission No.:	70 Keflavik, Iceland	Date Gathered:	4/4/68
Flight No.:	2	Date Analyzed:	4/22/68
Line No.:	Average	Altitude:	5,000 Ft.
Site No.:	166	Velocity:	---

Special Remarks: Water, Upwind-Downwind versus Crosswind

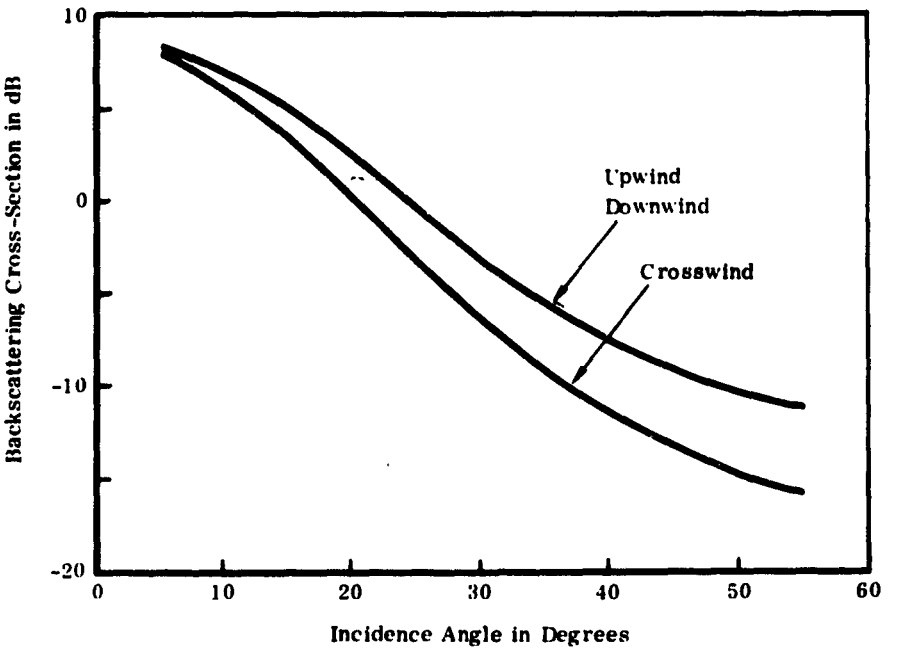

Figure 2-6 Comparison of Data Upwind-Downwind vs Crosswind

2.3 MISSION 72, SIGHT 167, FLIGHT 3, LINE 1, RUN 2A; LINE 1, RUN 2B AND LINE 2, RUN 1.

Mission 76, Site 167 was flown over the shallow region of Lake Mic'.igan, during May 1968. The primary purpose was to determine the effect that bottom-type plankton population, turbidity, wave refraction, and temperature have upon the accurate measuring of water depth by using multisensor data from shallow water of known depth.

Upon receipt of this computer processed data a mission report was requested. From the report it was determined that the data was gathered at 12,000 feet over the edge of Lake Michigan. The data, however, did not correlate with other over water missions. Figure 2-7 shows a comparison of previous over-water data with a mission 72 curve. Although the previous data is from a higher sea condition the shape serves to illustrate the problem with the Mission 72 curves. Further investigation showed that while the mission report stated the data was gathered with overland gain settings the actual mission logs showed it had been gathered with overwater settings.

This discrepancy was carried through to the computer where the data was processed with overland roll off instead of the correct overwater roll off. This explained the dynamic range problem so that the data was reprocessed with the overwater roll-off and made available for further analysis in mid-Semptember.

The extreme altitude of this mission affected the data beyond 40° incidence angle. The quickly-falling signal over smooth water at this altitude caused 400 Hz harmonic interference to bias the data.

2.4 MISSION 73, FLIGHT 1, SITE 130, LINES 8, 9, 10, 11, 12, AND 15.

Mission 73 was flown during the weeks of May 20 and May 27, 1968 over six California test sites. Site 130, South California, was chosen because it

Polarization:	V	Run No.:	2A
Frequency:	13.3GHz	Beam:	FORE
Mission No.:	72 Lake Michigan	Date Gathered:	5/7/68
Flight No.:	3	Date Analyzed:	8/29/68
Line No.:	1	Altitude:	12,000 Ft.
Site No.:	167	Velocity:	300 Ft./Sec.

Special Remarks: - - - - Mission 72 Data

——— Mission 34 (Gulfstream North) Comparative Curve

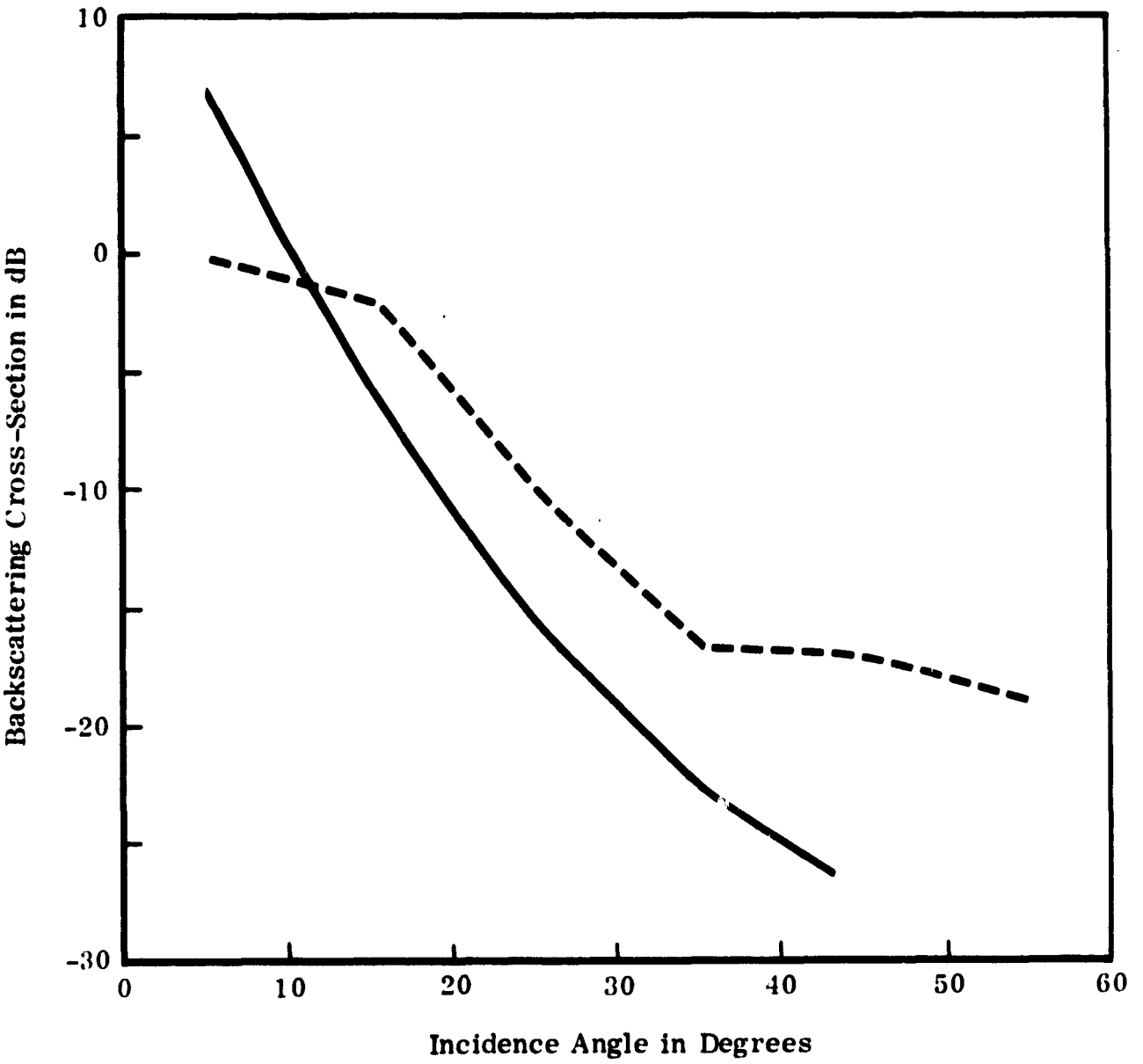

Figure 2-7 Comparison of Data

included variations in soil moisture conditions ranging from dry desert soil to completely saturated, recently irrigated fields. The flights were made to satisfy objectives within the disciplines of geology, geography, forestry, and hydrology. The results of the study were primarily for use in applying sensor/ground truth techniques to determine rural and urban land use, soil mositure, and surface heat balance.

This data was initially analog processed and released on a preliminary basis shortly after completion of the mission. The results of this quick look effort were specially helpful in determining that the primary goals of the mission had been accomplished.

After digitizing and computer processing were completed it was determined that the final processed data had been incorrectly time shifted. It was not possible to determine if the error had occurred during recent program modifications or it, in fact, the program was correct and the error was the result of recent system modifications which had not been interfaced with the data reduction group.

While the data was being recalled an adjustment was made in the program to correct the situation. The memo recalling the data suggested that investigators could apply hand calculations which would yield meaningful results from the information they had in hand. It was further suggested that the principal investigators select the lines of greatest interest to be reprocessed with the correction. Since this memo was written only line 8, run 1 from Mission 73, has been reprocessed. The results, received in raw filtered form were carefully checked and released for immediate distribution.

2.5 MISSION 74, FLIGHTS 1, 2, AND 4

Mission 74 was flown over four sites:

Site 76	Garden City, Kansas
Site 85	Lawrence, Kansas
Site 44	Purdue, Indiana
Site 168	Patuxent River, Maryland

The data collected was used to support agricultural and geographic land studies being carried on at the University of Kansas.

2.5.1 Flight 1, Site 76

A large part of the data gathered over site 76 during this mission was found to have exceeded the voltage limits of the aircraft tape recording unit. This was due to the occurrence of rain storms just prior to the over flights. Excessive saturation of the terrain and some surface water caused the return to exceed the calibration settings on the aircraft tape recorder. Had advance notice of this condition been received, the equipment could have been placed in the water roll-off mode and the data salvaged. Studies are still being made in an attempt to reclaim those sections where the data was not at the saturation level.

2.5.2 Flights 2 and 4

Data from flights 2 and 4 of Mission 74 were released with only minor qualifications. It was felt that this information was unbiased and could be used for further studies.

2.6 MISSION 75, FLIGHT 3, RUN 1 OF LINES 10, 11, 12.

The lines from which data has been reduced were flown over Weslaco, Texas. Data had been reduced from a previous mission over this area and the plots were compared. A satisfactory correlation was achieved and the data through 50° incidence angle were released to the Earth Resources Data Group.

2.7 MISSION 76 (25 LINES)

Test site 56, Mt. Lassen, was the area overflown during flights 4 and 5 of Mission 76. The area has a rough lavic and cinder topography and was flown to support geological studies being performed at the University of Nevada.

All lines requested (25 runs covering all of flights 4 and 5) included a short segment of data over Butte Lake (8-10 seconds). Since the system was in the overland mode those portions of each line over the lake saturated the on-board tape recorder. The data was computer processed before these areas could be isolated or table of times (see Table I) formulated specifying the areas to be disregarded in further analyses.

More detailed analyses detected large sections of each line which did not compare in shape, level, or dynamic range with past data over similar terrain. Figure 2-8 shows a comparison of the average and standard deviation curves from one Mission 76 line and one Mission 39 line over similar rough terrain.

Experience with past data had shown that better correlations could be expected between similar terrain types. Of particular interest in this figure is the curve shape of the Mission 76 data and the deviations from the average curve. Also, the drop in signal return at the higher angles is not characteristic of return from rough terrain and suggests a velocity variation not compensated for in data reduction. This compensation is difficult to make since accurate updates of aircraft parameters are not consistently available.

It should also be noted that due to certain changes being implemented in the computer program during the time this mission was being processed a 3 db factor was included in the program which could only be partially justified. This factor can affect the level of the data in the downward direction but not its shape or dynamic range. All lines except line 1, run 4 of Flight 4 contain this factor.

These points, (1) lack of correlation. (2) areas of tape recorder saturation, (3) excessive gain (x100) in the equipment for an overland mission at the relatively low altitude of 2200 feet and (4) the included computer factor lead to the release of this data with a qualifying memorandum. In the memorandum it was suggested that the data be studied closely and those

Polarization:	V	Run No.:	3
Frequency:	13.3GHz	Beam:	FORE
Mission No.:	76 Mount Lassen	Data Gathered:	7/18/68
Flight No.:	4	Date Analyzed:	8/1/68
Line No.:	2	Altitude:	2200 Ft.
Site No.:	56	Velocity:	284 Ft./Sec.

Special Remarks: ——— Mission 76 Fore Beam Average and Standard Dev.
- - - - Mission 39 (WSMR Lavic Line) Average and Standard Deviation

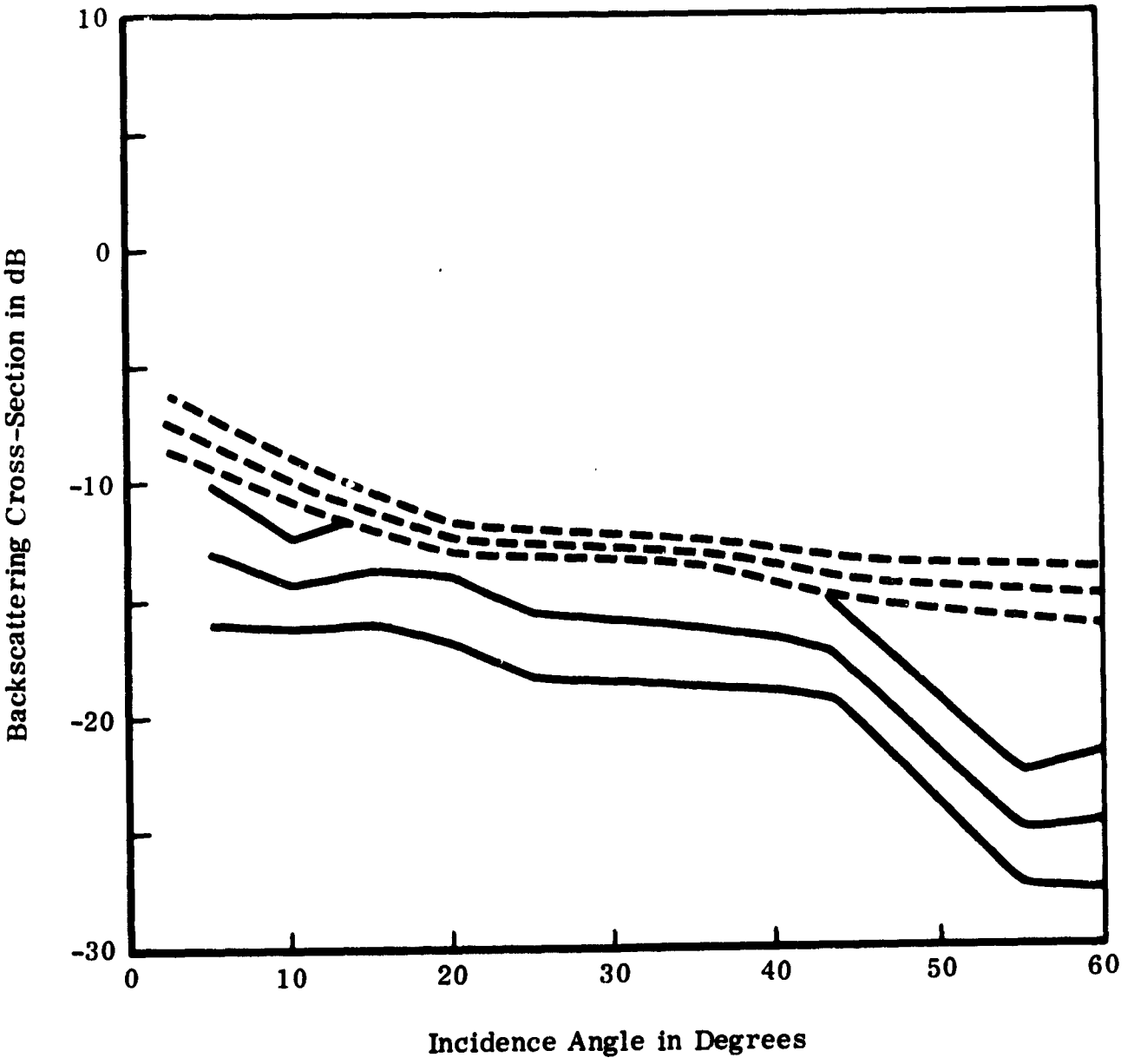

Figure 2-8 Comparison of Mission 76 Data and Mission 39 Data

lines of most significant interest be requested by the investigators to be reprocessed. Since the memorandum was transmitted most of the areas of concern have been clarified and the following lines have been reprocessed and released:

Flight 4	Flight 5
Line 1, Run 5	Line 2, Run 1
Line 1, Run 6	Line 2, Run 6

The only qualification placed on this data was that portion over the lake which saturated the aircraft recording system. See Table 2-2

2.8 MISSION 77, SITE 44, FLIGHT 2, LINE 31, RUN 1

Mission 77 was flown over site 44 on July 30, 1968. The flight was made in the Purdue University area near West Lafayette, Indiana. The objective was to gather 13.3 GHz scatterometer data for correlation with other sensor data gathered over the same area on Mission 74.

The flight log stated that a high gain setting of x100 was set in the system for the altitude 2000 feet at which this data was gathered. The millivolt levels of the recorded data are correspondingly high. The data, however, was collected with little or no saturation of the onboard tape recorder.

Processing proceeded smoothly with digital time histories being checked prior to final computer reduction. The data in the form of σ_o versus θ curves has been received and studied with satisfactory results. It should be noted that an error in the digital filtering portion of the computer program caused the data between 14:50:27 and 14:50:41 on the aft and between 14:50:41 and 14:50:42.5 on the fore to be erroneously plotted. The reflectivity plots between these times should not be used in further analysis of this data.

TABLE 2-2*

Areas of tape recorder saturation due to collection of overwater data with overland gain settings.

Mission 76, Site 56, Flight 4

Line 1, Run 1	18:27:19 - 18:27:27
Line 1, Run 2	18:32:53 - 18:33:00
Line 1, Run 3	18:38:58 - 18:39:06
Line 1, Run 4	18:45:54 - 18:46:04
Line 1, Run 5	18:52:35 - 18:52:44
Line 1, Run 6	18:59:03 - 18:59:13
Line 2, Run 1	19:06:30 - 19:06:40
Line 2, Run 2	19:13:28 - 19:13:36
Line 2, Run 3	19:20:29 - 19:20:35
Line 2, Run 4	19:27:35 - 19:27:42
Line 2, Run 5	19:33:41 - 19:33:47
Line 2, Run 6	19:40:18 - 19:40:24
Line 2, Run 7	19:47:13 - 19:47:19

Mission 76, Site 56, Flight 5

Line 1, Run 1	09:41:28 - 09:41:38
Line 1, Run 2	09:48:05 - 09:48:13
Line 1, Run 3	09:55:34 - 09:55:33
Line 1, Run 4	10:03:07 - 10:03:16
Line 1, Run 5	10:10:50 - 10:11:00
Line 2, Run 1	10:25:37 - 10:25:38
Line 2, Run 2	10:33:48 - 10:34:00
Line 2, Run 3	10:42:52 - 10:43:01
Line 2, Run 4	10:52:13 - 10:52:23
Line 2, Run 5	11:01:30 - 11:01:43
Line 2, Run 6	11:09:07 - 11:09:17

*The times for flight 4 were obtained by monitoring a dub of the original flight tape on an oscilloscope and rms meter. Flight 5 was not examined in the same way so that the times were determined from examination of the data curves.

From the available information it was possible to determine that a limited amount of saturation of the onboard tape recording unit had occurred. The data, however, indicated that the amount of biased information was not significant. One error in the digital filtering routine caused erroneous data to be plotted between 14:50:27 and 14:50:41 aft and between 14:50:41 and 14:50:42.5 fore. With these exceptions the data was released for distribution to the scientific community.

2.9 MISSION 80

The scatterometer data reduced from Mission 80 consisted of one line flown over site 76 (Garden City, Kansas). The information from flight 7, line 3, run 1, was received in four formats:

- Raw filtered voltages versus time
- σ_o versus θ plots
- σ_o versus time plots
- σ_o versus θ tabulations

It is known that this data was reduced while the computer program was still being checked out after initiation of modifications. These modifications left the absolute level of the data in doubt. A discrepancy of 3 db was noted between this data and data run prior to the program changes. The information did, however, show good character and would be of further value to the principal investigators so long as no conclusions were reached based on the position of the curve along the "y" axis.

Two other areas between 15:32:00 and 15:32:11 fore beam and 15:31:47 and 15:31:58 aft beam need to be disregarded during analysis since the data points are not properly plotted. The σ_o versus θ time plots show a single output value during these intervals. The conclusion is that the computer program did not properly consider the values within the time intervals noted. Further study into this situation was initiated.

2.10 MISSION 81, SITE 132, FLIGHT 9, LINE 1, RUN 1

Mission 81 was flown as part of the NASA Earth Resources Aircraft Program in support of four major scientific disciplines (hydrology, oceanography, geography, geology). The data from site 132, designated New Orleans, was requested by Northwestern University in support of studies being performed for the U.S. Geological Survey. The paramount objective of this particular study was to provide information on transportation and residential land use within the city.

The data requested from Mission 81 consisted of two minutes of data from flight 9, line 1, run 1, site 132. The scatterometer log labels this data line 1, run 3 in the mission report. It is felt, however, that line 1, run 1 is the correct designation and that data was actually collected from 20:20:37 to 20:24:30.

The data angles, noise floor and calibration level indicate proper system operation and valid data reduction procedures. Figure 2-9 shows areas of invariance where the signal is not changing. The following table lists the start and stop time of these irregular areas.

Start	Stop
20:22:20.7	20:22:21.7
20:22:24.3	20:22:26
20:22:28.2	20:22:29.3
20:22:35.3	20:22:37.3
20:22:43	20:22:45

These times are for the fore beam data only and serve as example as to the amount of data affected by this processing anomalie. The error will not be contained in any further data runs.

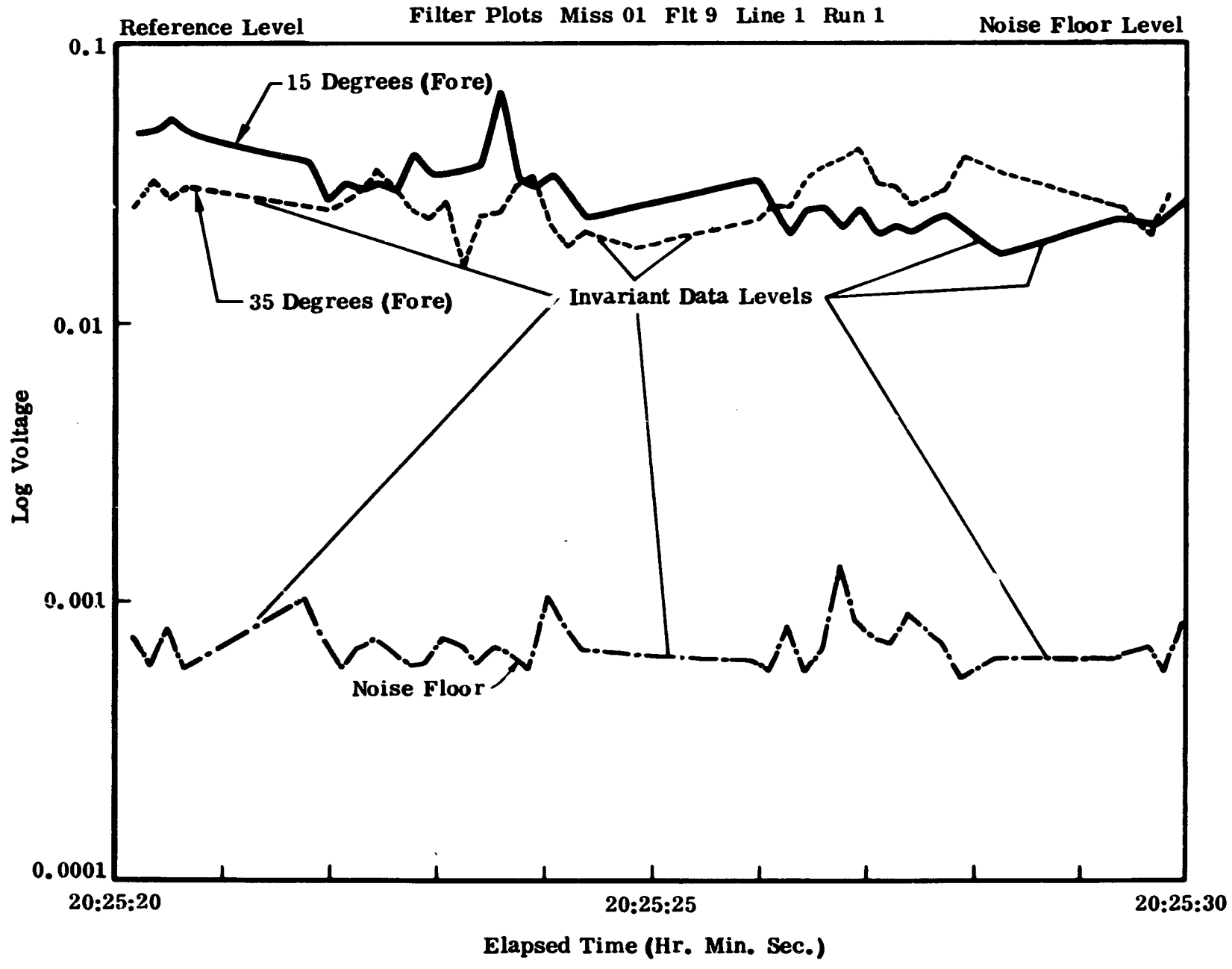

Figure 2-9 Scatterometer Data With Effects of a Data Reduction Anomalie

2.11 MISSION 88, SITE 184

Mission 88 was a combined agency effort with instrumented aircraft from the Manned Spacecraft Center, Goddard Space Flight Center and Naval Oceanographic Office in participation. The North Atlantic Ocean off the coast of Southwestern Ireland was the area of interest to be overflown. Studies were being conducted in support of the Oceanographic departments of New York University (Dr. Willard Pierson), and University of Kansas (Dr. Richard Moore). The primary and secondary objectives as stated in the mission plan are as follows:

- Primary Objectives:

  a. To obtain 0.4 GHz, 1.6 GHz, and 13.3 GHz radar scatterometer data over sea states in excess of 20 feet, concurrent with the Naval Oceanographic Office (NOO) airborne radar wave profiles.

  b. To obtain multifrequency radar scatterometer data over sea states below 20 feet at approximately 4-foot intervals concurrent with the NOO wave profiles.

  c. To obtain multifrequency radar scatterometer data over similar sea states with differing wind velocities, and over dissimilar sea states with the same wind velocity.

- Secondary Objectives:

  a. To obtain sea temperature data and determine the atmospheric effects on the data.

  b. Operational checkout of DPD-2 (side-looking radar), RS-14 (dual channel imager), and KA62 systems (multi-band camera).

No data has been released from Mission 88 as of this writing. However, several lines and runs are presently in various stages of processing. Table 2-3 gives the status of each of these lines. Based on quick-look analog verification it is felt that the quality of the data is good and should be useful to further oceanographic studies.

Mission 88 remains the most recent scatterometer mission from which data has been requested. At present, the scatterometer systems are in various stages of recalibration and checkout. For this reason, it is felt that upon completion of the Mission 88 data request, an effort will be made to go back to past mission and process lines of secondary interest in an attempt to compile a more complete library of σ_o versus θ curves over all types of terrain.

Table 2-3 Mission Data Reduction/Scatterometer Status as of 5-1-69

REQUEST	FLT	LINE	RUN	SCATT	ANALOG TO DIGITAL		GROUP I								GROUP II			
							ASG-90		VIBANA		FILTER PLOTS AND TABS		HARDCOPIES		REFLECT PLOTS AND TABS		HARDCOPIES	
					S	C	S	C	S	C	S	C	S	C	S	C	S	C
183	6	50	2	400	X	X	X	X	X	X								
184	6	50	3	13.3	X	X	X	X	X									
185	6	51	2	400	X	X	X	X	X	X	X	X	X	X				
186	6	51	2	13.3	X	X	X	X	X	X	X	X	X	X	X	X	X	
187	6	52	2	400	X	X	X	X	X	X	X	X	X	X	X	X	X	
188	6	52	2	13.3	X	X	X	X	X									
189	6	53	1	400	X	X	X	X	X	X	X	X	X	X	X	X		
190	6	53	1	13.3	X	X	X	X	X	X	X	X	X	X	X	X	X	
191	6	54	1	400	X	X	X	X	X	X	X	X	X	X	X	X	X	
192	6	54	1	13.3	X	X	X	X	X	X	X	X	X	X	X	X	X	
204	4	20	5	400	X	X	X	X	X	X	X	X	X	X	X	X	X	
205	4	20	5	13.3	X	X	X	X	X	X	X	X	X	X	X	X	X	
206	4	21	5	400	X	X	X	X	X	X	X	X	X	X	X	X	X	
207	4	21	5	13.3	X	X	X	X	X	X	X	X	X	X	X	X	X	
208	4	22	5	400	X	X	X	X	X	X	X	X	X	X	X	X	X	
209	4	22	5	13.3	X	X	X	X	X	X	X	X	X	X	X	X	X	

C = COMPLETED S = SUBMITTED

SECTION 3

PROGRAM CAPABILITIES

This section discusses the computer programs that are used in the reduction of scatterometer data from the 400 MHz, 1.6 and 13.3 GHz scatterometer systems. The format of the data output is similar for all systems. Therefore, only the current 13.3 GHz program capabilities are presented in detail. Those changes in the program which become necessary with the acquisition of the 1.6 GHz and 400 MHz system are also discussed.

3.1 OUTPUT FLEXIBILITY OF BASIC 13.3 GHz PROGRAM

The following listed data outputs are available to the principal investigators if requested.

- Time history plots of the filtered raw data.
- Time history tabulation of the filtered raw data.
- Time history plots of σ_o for each of the nine angles.
- Time history tabulations of σ_o for each of the nine angles.
- σ_o versus θ plots (fore and aft plotted separately).
- Up to 120 photograph number annotations. These numbers will correspond to their associated times.

Other options available to the principal investigators are as follows:

- Selection of up to 20 start-stop times within a given run.
- Selection of up to 20 start-stop times within a given run on the statistical reports.
- A time bias adjustment, should the photograph time differ from the IRIG time.

- Selection of up to 10 data bandwidths and the center frequencies for the fore beam and up to 10 for the aft beam data.
- The investigators may also select any time interval needed for definition, or may average several cells.

3.2 DISCUSSION OF 1.6 GHz AND 400 MHz PROGRAM REQUIREMENTS

The above capabilities and options are for the 13.3 GHz vertically polarized scatterometer system. The recent acquisition of the 1.6 GHz dual-polarized system requires additional features presently not available. The 1.6 GHz data can be computer-processed using the 13.3 GHz program with only slight modifications required to remove the sign-sensing portions from the filter. The digitizing rate will also be reduced from the 50K rate to a rate more in line with the 1.6 GHz data. Hence, simultaneous processing of all polarizations is feasible.

A 400 MHz computer program has been developed to reduce the forthcoming 400 MHz scatterometer data. The differences in systems design and data processing techniques justified this development of a new computer program.

One of the primary reasons a new program is necessary is the required variable doppler concept. The 13.3 GHz program measures a constant doppler frequency throughout a complete run and adjusts the angle (θ) for changes in forward velocity. This technique has been employed on the 13.3 GHz program to reduce some of those errors introduced by the inability of the analog filters to be frequently adjusted for velocity changes.

At the inception of the digital filtering it has become possible to update the doppler frequency to coincide with a constant angle (θ). The 400 MHz program was programmed to accomplish this fact by changing the frequencies to be filtered using the equation:

$$f_d = \frac{2V}{\lambda} \sin(\theta)$$

where:

f_d = doppler frequency to be filtered

V = aircraft forward velocity

λ = system wavelength

(θ) = angle to be measured.

The velocity component is to be updated through the use of an ASQ-90 system which can record flight parameters at 10/sec or 40/sec, either of which would be adequate. Vector analysis of the pitch angle and vertical velocity components will be accounted for in the filtering program.

Other considerations in the 400 MHz dual polarized program is the 400 MHz system duty cycle and the multipolarization capabilities. These modifications are lengthy and time consuming in the existing 13.3 GHz program. A 400 MHz program has been written and is presently in use.

Program capabilities and options available to investigators are:

- Lead card input of center frequencies.
- Lead card input of frequency bandwidths.
- Selection of data integration times in two parts.
- Selection of data start-stop times.
- Time history plots
- Power spectral density plot.
- Optional output in relative volts or decibels.

3.3 GENERAL DISCUSSION OF BASIC 13.3 GHz PROGRAM

Formal documentation of this 13.3 GHz program is found in Scatterometer Digital Filtering Program, FILTER, Report Number Q470, CAAD-NASA/MSC, by R. D. Rogan and J. L. Fisher.

The basic program is composed of three routines: FILTER, TIMTAB and REFLECT. FILTER computes the backscattered power within selected frequency bands.

The data is noise-like, with a near-Gaussian distribution. Two sidebands of doppler frequencies are folded into the range from 0 to 12.5 KHz on one channel, and again on a second channel with a linear 90° phase shift. The program unfolds the spectrum by modulating both channels to a higher center frequency and adding the modulated channels in quadrature. A Fourier transform is used to compute the frequency spectrum; adjacent spectral amplitudes are squared and summed in the desired frequency bands to simulate bandpass filtering with RMS averaging.

The two data channels are digitized at a rate of 25,000 samples per second per channel. The computer program changes count values from the analog-digital converters into voltage units.

To separate the forebeam data from the aftbeam data the following proce--dures were, until recently, followed:

- A linear interpolation was used to increase the sample rate to 100,000 samples per second on each channel.

- Modulated functions X and Y were formed by
  $X(n\Delta t) = CH_1(n\Delta t) * \cos(2\pi F_z n\Delta t) \quad n=0, 1, 2, \ldots, N-1$
  $Y(n\Delta t) = CH_2(n\Delta t) * \sin(2\pi F_z n\Delta t)$

where F_z = 12,500 Hz

Δt = time increment between samples

N = number of data samples over which to average

CH_1 = voltage samples from first (in-phase) channel

CH_2 = voltage sample from second phase-shifted) channel

- The sign-sensed function with separated sidebands was formed by $S(n\Delta t) = X(n\Delta t) + Y(n\Delta t)$.

NOTE

The sidebands are separated only if $CH_1(t)$ and $CH_2(t)$ are of equal gain. The RMS levels of both channels are computed at the beginning of each run, and a correction of up to 10% is applied to equalize the channels for the remaining data.

- The Fourier Transform F(S) was computed over a time interval T with a Fast Fourier Transform algorithm (Reference 1). The results are, as before, two sets of coefficients a_n and b_n for n=0, 1, 2, ..., N/2-1. The coefficients are "Hanned" to correct for filter leakage by

$$a_n = -0.25a_{n-1} + 0.5a_n - 0.25a_{n+1}, \quad n = 0, 1, 2, \ldots, N/2-1,$$

$$b_n = -0.25b_{n-1} + 0.5b_n - 0.25b_{n+1}.$$

Root-mean-square spectral amplitudes are computed by

$$A_n = 2\sqrt{a_n^2 + b_n^2}, \quad n = 0, 1, 2, \ldots, N/2 - 1.$$

- The harmonic numbers n are used to identify each amplitude A_n with a frequency F according to

$$n = F * T.$$

Then the output of NF filters is simulated by

$$P_i = \sum A_n^2 , \qquad i = 1, 2, 3, \ldots, NF,$$

with sums computed over each desired frequency range. After the filtering is completed for each period T, and advance in time is made, and the calculations are repeated. The interval T is the effective filter averaging time. An effective roll-off of 60 db/octave is attained in the case of the maximum T (8192 data samples) for this application. The spacing of the calculations may be specified to be greater than T, when desired, to reduce computing time.

A new method of separating forebeam data from aftbeam data has been recently developed by J. L. Fisher of the computation and Analysis Division, NASA/MSC, and present data reduction employs this new method. The derivation, written by Mr. Fisher, is included in Appendix A of this report.

To continue, a buffered binary tape is written with both forebeam and aft-beam data, designed for processing by the digital scatterometer data reduction program REFLECT.

The program REFLECT correlates the output of FILTER with the aircraft guidance and navigation parameters and computes σ_o for each of the nine angles both fore and aft, and, employing the SC4060 plotter, plots σ_o versus θ curves. A statistical average and standard derivation for requested time slices are also plotted with the angles. The program is documented in Advanced Digital Reflectivity Program, RFLTDG, Report Number TDR 825, by J. D. Garrett.

The third program for reducing scatterometer data is called TIMTAB. This program computes reflection cell centers, the times of intersections of the aircraft path with imaginary lines at nominal angles to the vertical, and cell center times. The program constructs a time table which is used

in REFLECT and FILTER to determine the sampling of the scatterometer data. The program is reported in Scatterometer Time Table Computations, TIMTAB, Report Number TDR 440, by J. D. Garrett.

The data is finally plotted in one of the formats described earlier and released as hard copies in book form. Careful study is made of the output to insure its quality prior to releasing it to the scientific community.

SECTION 4

SCATTEROMETER DATA DISPLAY USING THE SPATIALLY ADJUSTED TIME HISTORY PLOT

For several years, the NASA Earth Resources Program has collected scatterometer data over land areas and the sea. During this time the data processing techniques were constantly refined to upgrade the quality of the data and to display the data in a form most usable to investigators. As more investigators became aware of the value of scatterometer data, additional data displays were developed to best fit their needs. The development of scatterometers with multipolarization capabilities and/or operating at different frequencies will increase, even more, the amount and worth of scatterometer data to the Principal Investigator. This increase of data will require that efficient handling and display techniques continue to be developed to furnish the principal investigators maximum efficiency with the best information for qualitiative and quantitative analysis of land and sea areas.

Present data display techniques consist of σ_o versus θ plots. These plots are now used to illustrate all kinds of data whether it be over land, ice, snow or water; whether the terrain be homogeneous or inhomogeneous. Since each investigator is concerned with the needs of his own scientific discipline, the σ_o versus θ plot does not necessarily help him. The oceanographer, for example, is interested in data that is averaged over many data samples, and the σ_o versus θ plot is perhaps exactly what he is looking for. However, the geologist is interested in abrupt changes in terrain such as fault lines or transition areas between geological terrain types, might find that the σ_o versus θ plot is of little help.

In an effort to meet the demands of efficient data handling, a technique of data display was developed that would supply the investigator with more useful information. This technique of display is called the Spatially

Adjusted Time History (SATH) plot, and is illustrated in Figures 4-1 and 4-2. Much of the information about the terrain which was obtained in the past with various aircraft remote sensors was presented by statistical rather than discrete parameters. The radar backscattering cross section are examples of such statistical information. The possibilities of identifying certain pertinent ground features is limited by the application of such information. When details of ground features, or its composition, are determined by using such information, the results are said to be effective, compromised, or averaged results. When the facts are reviewed it is found that valid statistical information was presented; however, in many cases what was actually desired was nonstatistical information - or discrete detail of the surface. The "discreteness" of the ground parameters can be vastly improved by the SATH process by increasing the resolution of the system and by assimilating all the contained information through various techniques - correlation is one such technique.

It should be pointed out that the SATH plot is most advantageous over inhomogeneous terrain. The σ_o versus θ plot is probably still best for over water data.

The SATH plot offers the following advantages:

- It presents an overall display of a complete line of data to the investigator. Figure 4-1 is a SATH plot of Mission 73, Site 130, line 12 aligned with a photographic mosaic of the same area. Although the SATH plot would consist of several lines of data representing different angles, all of which would be time adjusted to a single ground point, the data illustrated in Figure 4-1 represents only one angle ($\theta = 20^\circ$) for clarity of presentation. This line represents the data that has been digitally filtered and averaged at one second intervals. The one-second time interval in this case was arbitrary and selected for purposes of presentation only. The time interval used in an overall SATH plot is a function of the velocity of the aircraft, the type of terrain involved, and the objective of the flight (agricultural, geological, etc.). Smaller time intervals such as 0.5 second in

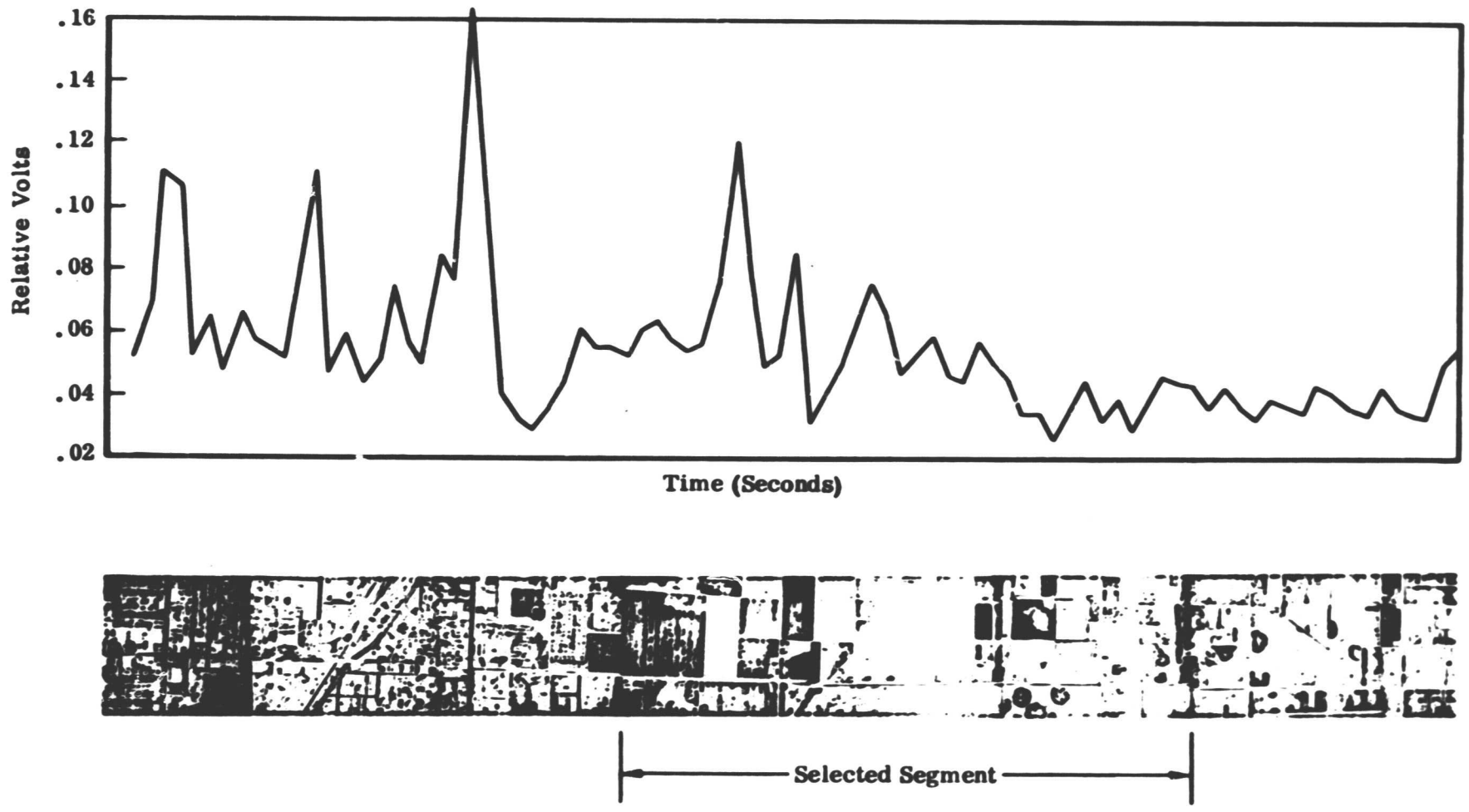

Figure 4-1 SATH Plot Data Averaged Every 1.0 Second

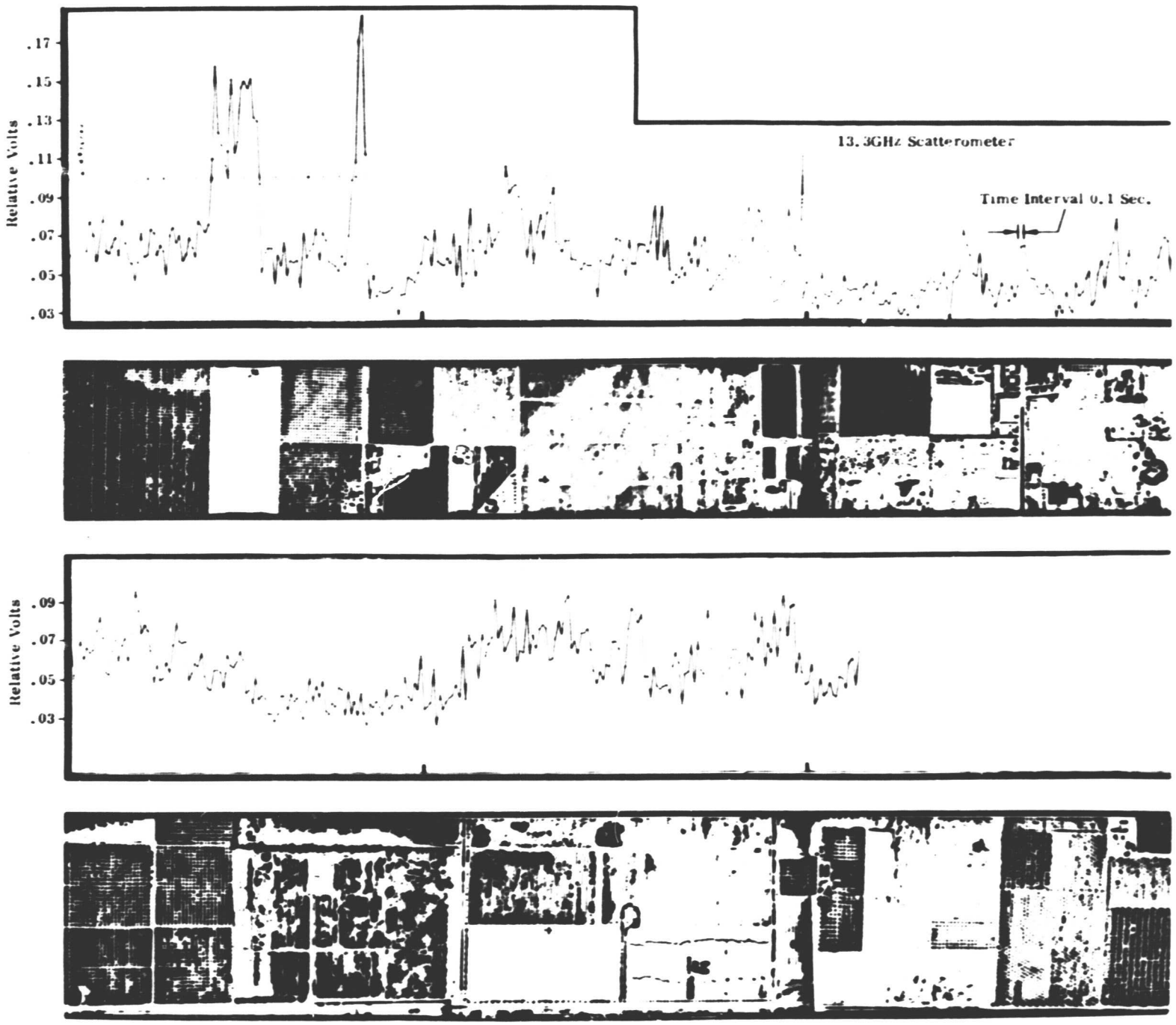

Figure 4-2 SATH Plot With 0.1 Second Sampling

many cases has proven to display the data satisfactorily. The amount of computer time required by the digital filtering program at this rate, however, would be increased accordingly.

- It allows the investigator to be selective in requisitioning detailed data from NASA. The investigator can select from Figure 4-1, those portions of the data that exhibit features warranting detailed study. These selected portions may be presented in a similar SATH plot at a higher sampling rate. An illustration of this is shown in Figure 4-2, where a time interval of 0.1 seconds is used for a selected segment of data. Thus computer time can be more efficiently utilized by being selective in processing data rather than processing the entire line of data at a high and costly data rate.

- It provides the capability of specifically locating near-homogeneous data for computing σ_o values within an entire line of data. The present method of computing σ_o values of terrain such as Mission 73, is to compute σ_o values for the whole line. The SATH plot as shown in Figure 4-1 will enable the investigator to select specific data, corresponding to near-homogeneous terrain, with which to compute an average σ_o value. An example of such near-homogeneous terrain is illustrated at the beginning of the photograph of Figure 4-1 where an orchard is shown preceding a plowed field. The data corresponding to this area should be used to compute an average σ_o value of this area. The same process can be applied to the plowed field, or other specific features. Thus the SATH presentation enables one to compute σ_o values more definitively and efficiently.

Figure 4-3 shows the scatterometer data collected at three angles and spatially adjusted. This data represents the same terrain shown in Figures 4-1 and 4-2. Note how the characteristic hump on the data appears

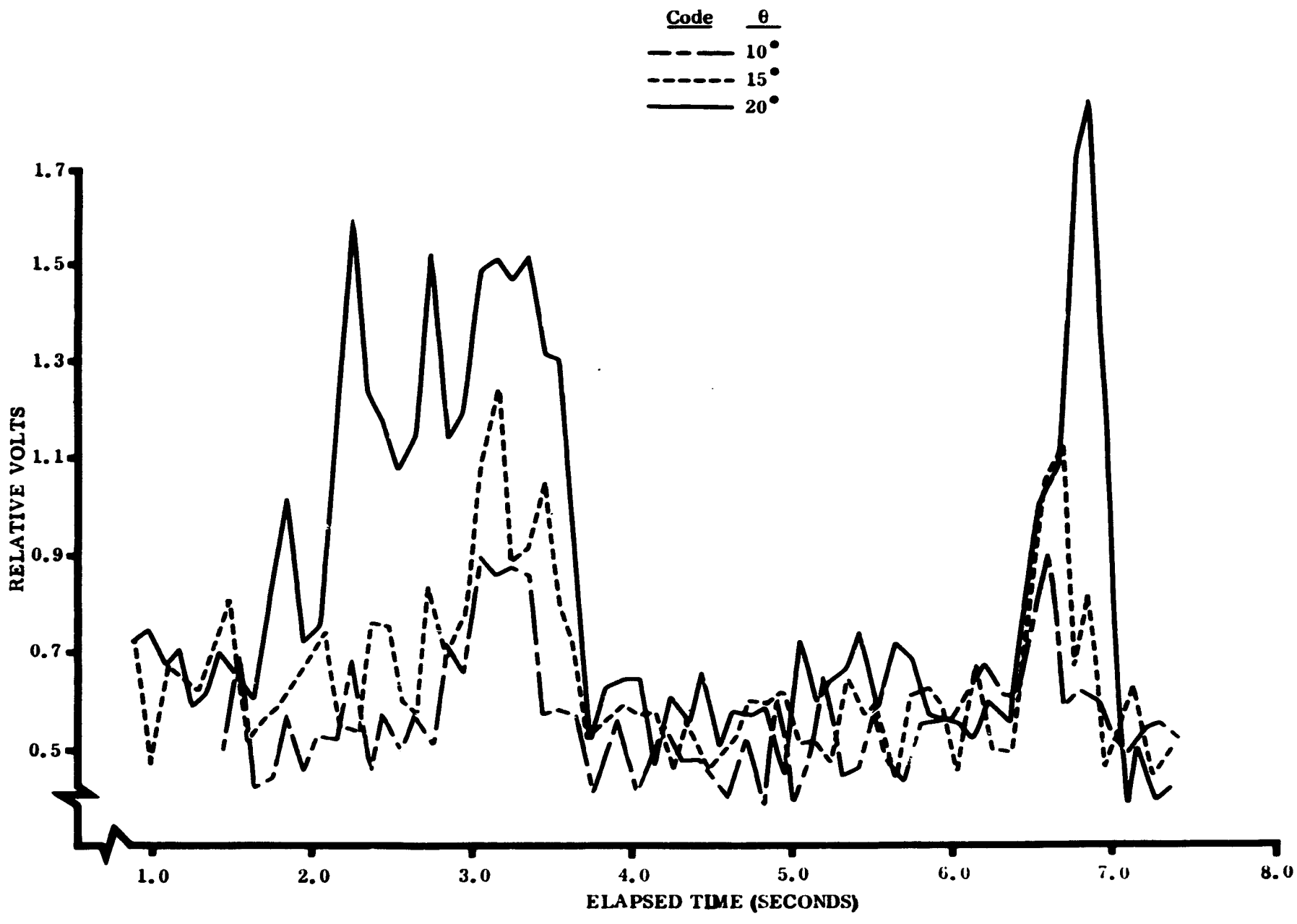

Figure 4-3 Data Collected at 3 Angles and Spatially Adjusted

in all three angles at time 3 to 4 seconds. This feature would illustrate to the principal investigator how the electromagnetic energy return level changes with angular return. The SATH technique of display emphasizes such areas of terrain characteristics over a complete line of data.

Another example of this is shown in Figure 4-4 representing a segment of data from Mission 76. This line crossed a small body of water which is clearly illustrated in the data by the large return at time 40 to 50 seconds. Note how the data behaves as a function of angular return. The "inversion" point characteristic of over water data is clearly visible in this representation. The insert at the upper right of Figure 4-4 is a σ_o versus θ plot made of this data and averaged over the width (or time interval) of the characteristic "hump" enhanced by the SATH format.

The implementation of the SATH format will involve computer programming on the SC4060 computer-plotter. The data from each angle can be time adjusted through a geometrical translation to a single reference point. The independent (time) variable can be printed out to correspond with the 9 inch x 9 inch photograph by utilizing the aircraft velocity data. The SC4060 can be programmed to print the independent variable to correspond to any desired photograph length through this process. Utilization of the better frame capability of the SC4060 will provide a continuous plot of data. The final product can be stored on microfilm.

It is felt that the above described SATH technique will provide a more efficient tool to the principal investigator by allowing him to edit the overall data of a specific terrain and select specific areas of interest for more detailed analysis. The technique will also permit NASA to utilize computer time associated with the costly digital filtering program more efficiently. The bulk of data printed will be reduced accordingly. It is suggested that the overwater data continue to be displayed as σ_o versus θ plots since the SATH format at this time does not seem to offer a greater advantage in this area.

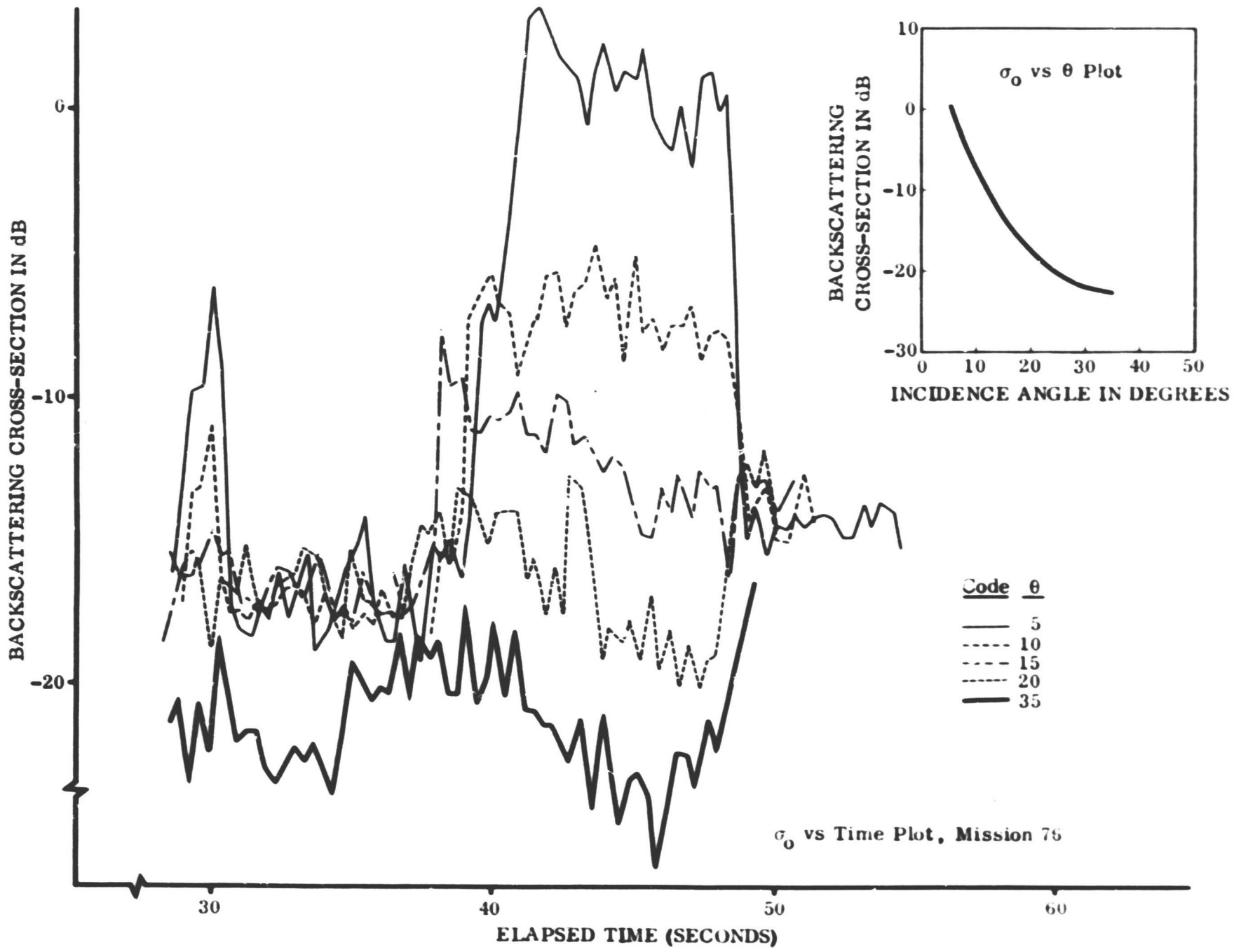

Figure 4-4 Segment of Data From Mission 76

Further studies in the area of data output formats should continue. It is necessary that efforts continue to be expended to derive new methods of remote sensor data display so as to enhance its usefulness to the entire scientific community. The efforts should point toward identifying the most basic data forms for each sensor in order that direct comparisons between sensor can be achieved.

SECTION 5

DATA VALIDATION

Since the inception of the NASA Earth Resources Survey Program an enormous volume of data has been collected from the 13.3 GHz scatterometer. Investigators are requesting an increasing amount of this data to be processed. The new dual-polarized 13.3 GHz scatterometer and the 1.6 GHz scatterometer will increase the amount of data collected in future missions and an increase in requests for data from user groups can be expected.

The data processing load, if data validation procedures and optimization techniques are not implemented into the data processing programs, will cause much of the usefulness of this valuable data to be lost because of the inability to process it in time to meet the requirement of the scientific community.

This section presents a study of the present data validation procedures and suggests methods of automatic editing which will, if implemented, help speed the transmission of data to the investigators.

The present verification process is separable into three main areas:

- Pre-Mission verification
- Post-Mission verification
- Final computer output verification

An automatic data editing program can be implemented in the post-mission phase of the validation and will allow phases two and three of the process to be handled entirely on the digital computer. This will increase the efficiency of the data verification procedure so that regardless of the

amount of data requiring reduction, a minimum turn around time can be maintained on all requests. Such an automatic computer program is described in Appendix B.

This section also includes an introduction to the 13.3 GHz single polarized scatterometer system as well as a breakdown of the verification process as it has been applied to the data.

At this point, a brief description of the present 13.3 GHz, single polarized, scatterometer and data collection system is appropriate.

5.1 13.3 GHz SCATTEROMETER SYSTEM

Figure 5-1 is a block diagram of the 13.3 GHz scatterometer. The transmitting antenna radiates a broad beam (approximately 120 degrees) along the fore-aft axis of the aircraft and a narrow beam (approximately 2.5 degrees) along the port-starboard axis of the aircraft. The receiving antenna is identical to the transmitting antenna which makes the two-way beamwidth about 100 degrees by 2.5 degrees.

As the aircraft is flown, data is received from all angles of incidence simultaneously. The data is detected by a direct-to-audio technique and amplified. It is then collected on two channels in phase quadrature and recorded on an onboard FM tape recorder. Splitting the received data into quadrature pairs is done for the purpose of later combining the two channels in a single sideband modulator to separate the forward doppler spectrum from the aft spectrum. Also on one channel, a ferrite modulator enables the insertion of a calibration signal that is independent of all other system parameters. All the collected data is then referenced to the calibrate signal during data reduction with the result that an absolute power level reference is defined for every data point on the finalized output.

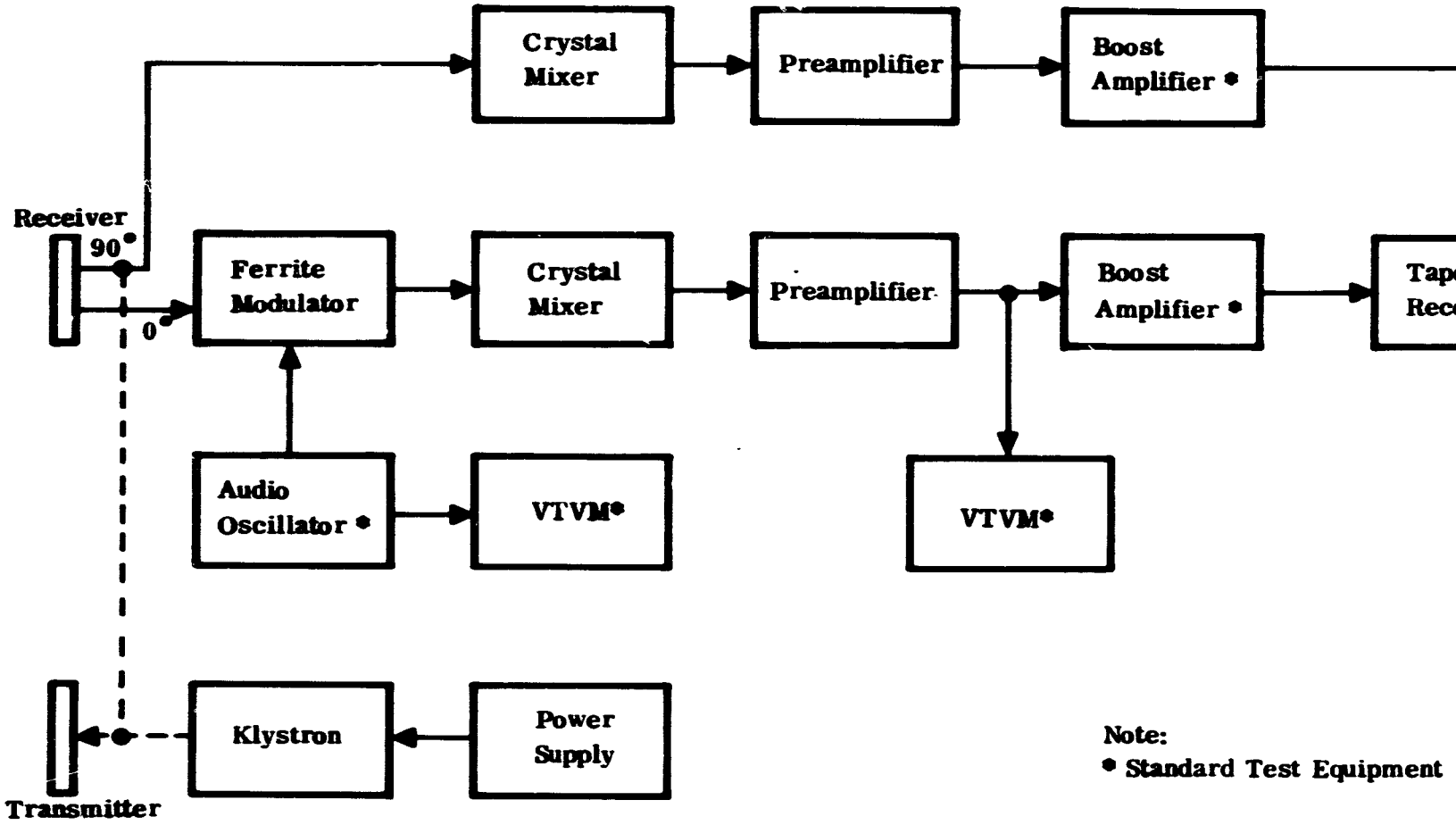

Figure 5-1 REDOP Block Diagram

5.2 PRE-MISSION CHECK PROCEDURES

The main purpose of the pre-mission check is to ascertain if the equipment is operating properly. Test data is collected in a flight over a prescribed area covering both land and water. The information is reduced immediately using quick-look analog reduction techniques. To isolate equipment errors the reduction process is accomplished in two different formats, Power Spectral Density (PSD) plots and Time History (TH) plots.

To detect frequency interference and other system problems, the PSD's are made from one second analog data tape loops and played back on a look recorder and through a sweep-filter power spectral analyzer. The sweep oscillator on the analyzer produces a continuous output, through a log converter and X-Y recorder, of signal amplitude versus frequency. A block diagram of the process and an example of a PSD are shown in Figures 5-2 and 5-3.

The TH's are made by tuning the oscillator of the spectral analyzer to particular frequencies corresponding to specific incident angles.* The data tape is played through the analyzer and a plot of signal amplitude versus time produced by a pen recorder. Several time histories of signal amplitude are usually produced over the same data by running the tape back, resetting the analyzer and plotting. It is the usual case when selecting a set of frequencies for plotting to include the calibrate signal frequency and a frequency far enough beyond the systems signal range to represent system noise floor. A block diagram of the time history procedure appears in Figure 5-4.

---

* Frequency and angle are related through doppler frequency equation $f_d = \frac{2V}{\lambda} \sin \theta$.

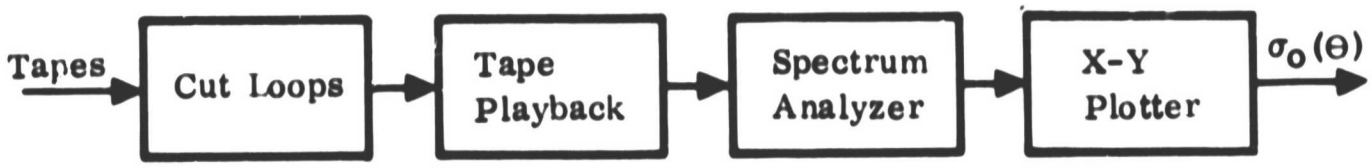

Figure 5-2 Tape Loop Data Analysis Technique

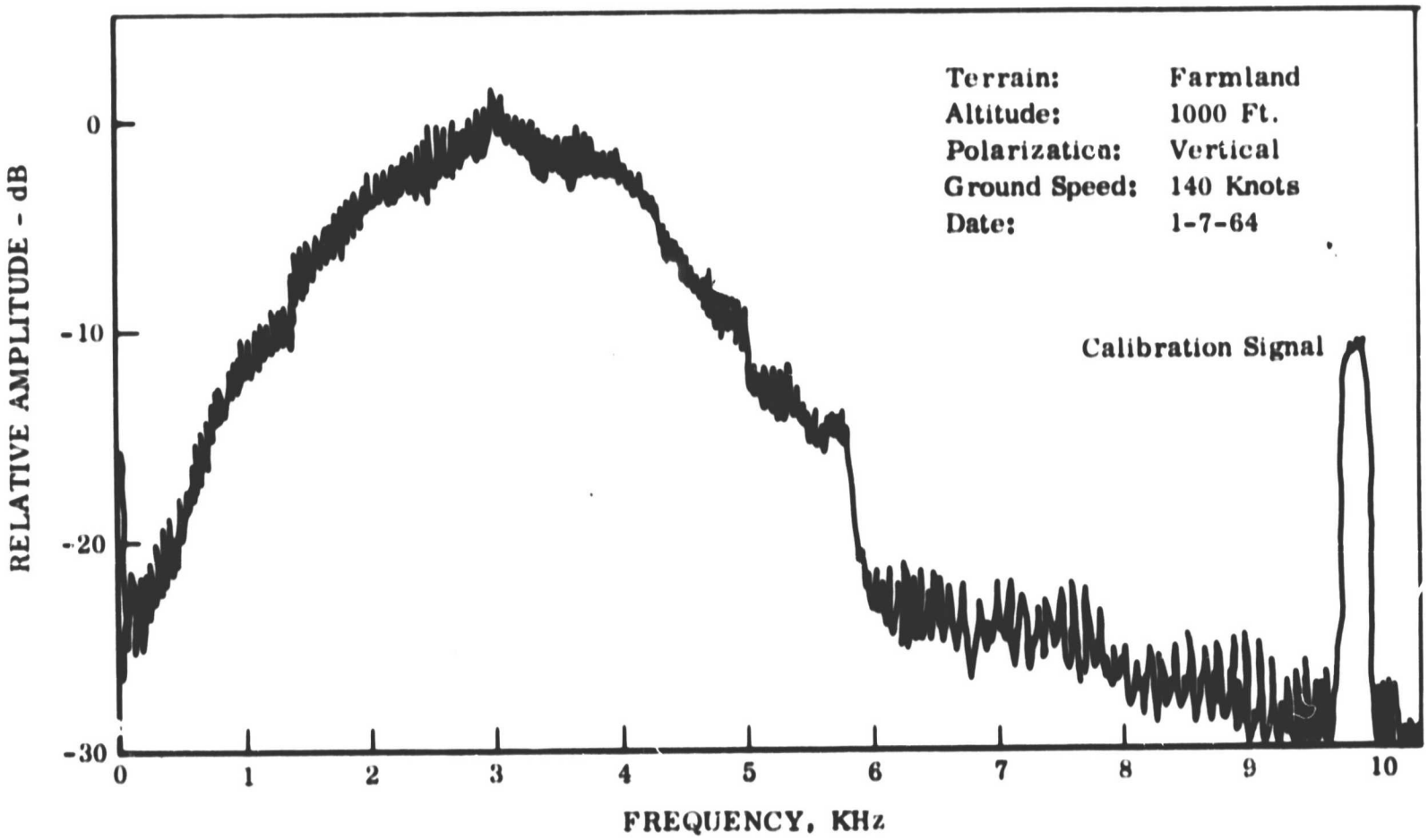

Figure 5-3 Typical Overland Frequency Spectrum

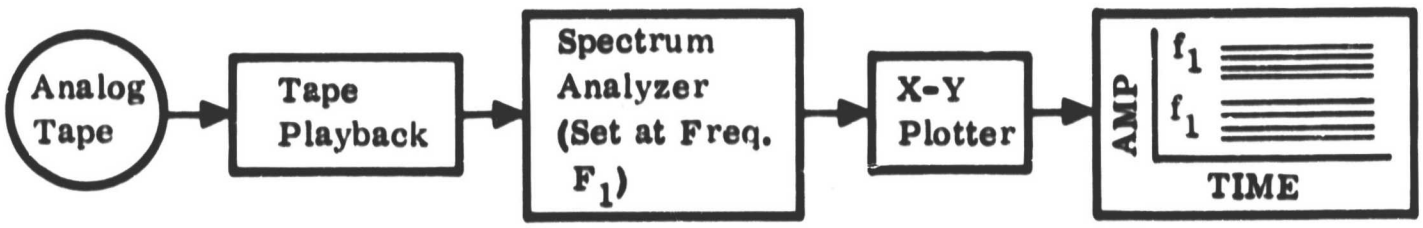

Figure 5-4 Time History Data Analysis Technique

The PSD's and TH's are studied to determine if variations in the data are valid ground return signals for the test area flown or are indicative of equipment malfunctions. Past experience with the data over the same and similar terrains and comparisons with theoretically expected returns for the test terrain are used in determining the validity of that data.

Since it is often difficult to determine if a particular data variation is a function of terrain or is a system problem, system tests are performed on the ground. The equipment is placed in an operational mode but the antenna is prevented from radiating by the placement of Echosorb over its elements. Only the internal system noise level is recorded without the uncertainty of actual reflected data. After recording, this information is played back through an analyzer and studied in the same manner as previously described PSD's or TH's.

There are three advantages to beginning the verification process at this pre-mission phase:

- Provides information for detection of system problems so that repair, modification or adjustment to correct these problems can be initiated prior to a mission.

- Provides information for formulation of a data reduction plan for mission data which could circumvent or correct for those problems which could not be adjusted prior to the mission.

- Provides data to compare with post-mission test data to determine what, if any, additional problems occurred during the mission.

5.3 POST-MISSION VERIFICATION PROCEDURES

A similar quick-look analog check of the data should be made routinely upon return of the aircraft from an actual mission. The actual post mission phase of verification, however, is a digital process. It is in this area that the greatest savings in time and cost could be realized with an automatic data validation and editing program. The emphasis in this phase is on the quality of the data collected and the determination of the optimum procedures for final data reduction.

In the past, data quality has been checked by reduction of analog and/or digital PSD's and TH's. The study of these plots made it possible to identify specific problem areas and to recommend optimum data reduction procedures. This method has shown certain weaknesses as a result of the increased volumes of data being requested and reduced. During peak periods computer time becomes critical and as much data as possible is reduced during each available processing interval. This reduction is usually accomplished without regard to any problems which may require special processing procedures.

There is a time lag between the production and study of PSD's and TH's and the resulting recommendations for data reduction. In the past some data was needed by investigators before the validation checks were completed. This resulted in the processing of some invalid data which was costly in terms of the computer time. The years of experience with scatterometer data must be formulated and incorporated into an automatic data editing program to combine editing and processing into a single step which would eliminate the reduction of bad data.

Some of the types of problems identified in the past are outlined in Table 5-1. Examples of these problems as they appear in analog processing are displayed in Appendix C, which also describes the methods used in recovering such data during processing.

TABLE 5-1

PROBLEM CATEGORIES	CONTRIBUTING FACTORS PREVIOUSLY ISOLATED	VARIATION NOTED IN DATA (SEE APPENDIX A FOR EXAMPLES)
(1) 60 Hz Interference (When system operated on 60 Hz power)	60 Hz power supply ripple	Large spike at 60 Hz noted in PSD spikes of 60 Hz harmonics at other frequencies
(2) 400 Hz Interference	(a) Inadequate cable shielding and other wiring problems (b) Inadequate aircraft ground connections (c) Faulty patch panel connections (d) 400 Hz power supply ripple	(a) Large spike at 400 Hz on PSD spikes of 400 Hz harmonics at other frequencies (b) Poor overall dynamic range noted in both PSD and time histories.
(3) Excessively high noise level	(a) Bad crystal diode (b) Improper equipment operation during data playback procedure (c) Improper tape recorder operation during tape dubbing procedure (d) Improper gain factor used in equipment during data collection causes tape recorder saturation onboard aircraft	(a) Poor dynamic range on PSD's and time histories. Range measured from highest signal to noise floor less than 20 db. (b) db level at 9 KHz is higher than the level at a frequency less than 9 KHz on time history (c) 9 KHz noise floor follows signal at other frequencies on time histories.

TABLE 5-1 (Continued)

PROBLEM CATEGORIES	CONTRIBUTING FACTORS PREVIOUSLY ISOLATED	VARIATION NOTED IN DATA (SEE APPENDIX A FOR EXAMPLES)
(4) Poorly defined calibrate signal level	(a) Lack of accurate speed control on data playback recorder	(a) Ragged 10 KHz spike with rounded peak as plotted on PSD.
	(b) Shut down of onboard equipment in middle of data collector	(b) Drop out of cal signal; periodic spikes on the cal signal; no cal signal at all as plotted versus time on time history.
	(c) Loose connection to the audio oscillator onboard aircraft	(c) Excessive variations in the cal signal of more than ± 3db for long periods of time noted on time history.
	(d) Saturation onboard tape recorder due to gain setting in overland mode and data collected over water	
(5) Periodic noise spikes which	RC-8 camera's intervolameter pulsing circuit being picked up through faulty patch panel connection	Spike 5 to 6 db in amplitude appear most strongly in 9 KHz noise floor as plotted on time history. These spikes occur through the data at intervals from 5 to 10 seconds long depending on aircraft altitude.

TABLE 5-1 (Continued)

PROBLEM CATEGORIES	CONTRIBUTING FACTOR PREVIOUSLY ISOLATED	VARIATION NOTED IN DATA (SEE APPENDIX A FOR EXAMPLES)
(6) Oscillations and periodic interference	(a) Land based control radar tracking aircraft and being picked up on data channel	(a) Areas in data of few seconds duration which occurs in both channels as a periodic pattern. When viewed on oscilloscope these areas show sinusoidal characteristics with high millivolt levels.
	(b) Operation of equipment at extreme altitudes.	(b) Periodic oscillations or interference patterns that are similar to those mentioned in (a) but occur in one channel only.
	(c) Poor transistor socket connections in equipment	(c) An interference pattern noted on PSD's at between 7 and 8 KHz. Appears as a buildup in signal level which falls off beyond this point.
	(d) Possible propeller modulation being picked up at antenna	
	(e) Possible resonant frequency vibration of internal or external airframes section being picked up in data	

It is obvious from these examples that by generating digital PSD's and TH's and checking them internally this phase of data verification can become entirely automated.

5.4 GENERATION OF DIGITAL PSD's

400 Hz and 400-Hz harmonic interference has been one of the biggest problems associated with the determination of data quality. To recognize such interference and to determine the data quality in the presence of this interference is of prime importance. The generation of a PSD would display the data as a function of frequency and thereby enable identification of the interference spectrum.

The traditional method for calculating the power spectral density function i.e., the power per unit cycle in a signal has been to take the cosine Fourier transform of the autocorrelation function. Mathematically, if $G_R(F)$ is the power spectral density function evaluated at specific frequency increments then:

$$G_R(F) = 2h \left[R_o + 2\sum_{r=1}^{m-1} R_r \cos\left(\frac{\pi_r f}{f_c}\right) + R_m \cos\left(\frac{\pi\, mf}{f_c}\right) \right]$$

where $F = n \cdot \Delta f$, $n = 0, 1, 2, \ldots, m$

h = time increment between data values

R_r = autocorrelation function*

F_c = cut off frequency $\frac{1}{2h}$

Δf = specified frequency

* Autocorrelation Function R_r can be defined as

$$R_r = \frac{1}{N-4} \sum_{n=1}^{n-r} X_n \cdot X_{n+r} \quad r = \text{lag number} = 0,1,2,\ldots,m$$

N = number of data values $\qquad$ X_n = Adjusted data value $(X_n - \bar{X})$

X = mean of data values $\qquad$ m = maximum lag number

more simply, if P_i is the power in a frequency band BW about a discrete frequency, f_i, the power spectral density at that frequency and bandwidth can be defined as:

$$G_i = \frac{P_i}{BW}$$

By applying the Fast Fourier Transform Algorithm the power in any band is readily determined since

$$P_{f_i}(BW) = \sum_{f=f_i-\frac{BW}{2}}^{f_i+\frac{BW}{2}} A^2(f)$$

where $P_{f_i}(BW)$ = Power in band of BW centered at F_i.

$A^2(f)$ = Squared Fourier amplitude for frequency f.

G_i is then calculated from the P_{f_i} values by dividing by BW. A PSD computed within each 18-second segment of digitized data would be sufficient to yield a sample spectra for each mile of terrain along the flight path. This sample rate will be made flexible to enable computations to be made more or less frequently when desired. Each plot would be a function of frequency from zero Hz to slightly beyond the calibrate signal frequency.

Once generated, the PSD format can serve as the basis for the application of statistical techniques to determine the extent of unwanted interference in the signal.

To begin the sequence of tests, each plot will first be defined by a best fit polynominal. Pre-programmed routines are available for the application of this technique which involves selecting a polynominal of the form

$$Y(X) = \sum_{n=o}^{N} a_n X^n$$

and adjusting the coefficients a_n to minimize the expression

$$D^2 = \sum_{m=1}^{M} D_m^2$$

where the D_m are the difference between the measured data (values of the PSD) and the polynominal ordinate at the M points X_m, m = 1, M. In practice the order of the polynominal, N, is chosen such that N<<M (N = 3 can serve as a first estimate to this polynominal in this particular application).

With the PSD defined by a best fit curve it will be possible to check for variations of the individual data points about this curve and a tabulation made of the points with a variance from the nominal of greater than ±4 db. If more than eleven* such variations are noted within the frequency bank from 0 to 6 GHz the data can be rejected and further examinations made. The results of this test can be used to determine if further tests are required. Such tests would include a measurement of signal dynamic range (range of the peak signal to the noise) and a measurement of the relative position of the noise with respect to the calibrate signal power reference level.

5.5 DYNAMIC RANGE

The dynamic range of the signal can be determined automatically by identifying the coordinates with the largest and smallest "y" components during computation of the best fit curve mentioned previously. Identifying the abscissa or "x" component yields the frequencies at which the high and low values occurred. A relative comparison of these two ordinates is a measure of the dynamic range of the signal. A dynamic range of less than 18 db would require further study of the data.

---

* This is a first estimate (based on past experience) of the number of bad data points required to invalidate the data within this frequency band. Experience with the testing procedure will yield an optimum value. This is true of all actual values used in this document.

5.6 TIME HISTORIES

A series of tests designed to provide information about the stability of the data as a function of time can be implemented at the time of digital filtering. Costly computer time can be saved if these tests are designed to stop the filtering process when data is of poor quality in terms of its stability with time. An alternate procedure would be to implement the checks after filtering but prior to final processing in the REFLECT portion of the present program. This system would also provide the means for reducing processing time and costs.

The testing consists of monitoring the voltage levels at the outputs of the digital filters and performing comparative analyses with these monitored levels. Individual checks will be made of the 10 KHz (nominal) calibrate signal and the 9 KHz (nominal) noise floor level. The information obtained from monitoring these two signals will be used to check their stability over particular time intervals and to determine their positions relative to each other.

The output of the calibration or reference filter can be sampled for a Δt time interval. A straight line can then be fitted to this data and a tabulation made of those points varying from the nominal by more than ± 2 db. The criterion for examining the data more closely would be for the number of points outside the limits to exceed eight (8) in one 15-second Δt. If each such interval is identified, the data within them can be excluded from further processing. The editing program can further be designed to stop the filtering process when the number of extreme points becomes excessive in three or more successive Δt intervals.

Using the outputs from the noise floor filter, a similar test can be desgined to determine its stability. Combining the two tests can be considered such that before stopping the filter program, excessive variations would have to appear in corresponding intervals on both the calibration and noise floor channels.

5.7 PEAK CALIBRATE LEVEL TO NOISE MEASUREMENT

The position of the noise floor relative to the peak calibration power level is of importance in determining data quality. A relative difference of less than 15 db suggests a high noise level or a poorly defined calibrate signal either of which can be indicative of multiple system problems, as shown in Table 5-1.

The test for measuring this relative difference can be done in parallel with the above stability check.

In this case the voltages monitored over the Δt intervals would be averaged and the ratio $\overline{E}_n / \overline{E}_R$ computed, where $\overline{E}_i$ represents the average voltage from the noise floor filter and $\overline{E}_R$ that of the reference signal filter. A relative difference in decibels is found with the logarithmic equation:

$$\text{Relative Voltage Difference} = 20 \log \overline{E}_n/\overline{E}_R$$

If this ratio, which may need to be computed only every fourth Δt, is found to be less than -18 db* for any one sample the interval's time is tabulated. These intervals then do not enter into final processing without further examination. As before, the filtering process can be stopped completely to compensate for the extreme situation where several successive intervals fail the test.

5.8 CONCLUSIONS

The above represent ideas about the types of tests which will be required to determine the feasibility of a data editing and validation program. They are the extension to the computer of the processes presently applied manually to check the quality of the scatterometer data.

---

* Minus sign signifies $E_n > E_R$

To implement a trial program, it will be necessary to have data on magnetic tape in raw digitized form sampled at the presently-used rate of 25 KHz per channel. Also required on tape will be data in raw filtered form at the output of the present digital filtering system.

Once feasibility is proven and such a program is integrated into the present computer processing system, the entire second phase of the validation procedure would be entirely automated.

APPENDIX A

DERIVATION OF SIGN SENSING ROUTINE

BY J. L. FISHER NASA/MSC

SIGN-SENSING

A DIGITAL SOLUTION IN THE FREQUENCY DOMAIN

It will be shown that sign-sensing can be eliminated altogether and that the positive and negative doppler sidebands can be separated by simple interpretation of the Fourier Transforms already being used in obtaining the doppler spectrum. No interpolation will be required.

The sequence of processing the digital time-series of data values representing an "integration period" is read into the computer memory, the necessary calculations are performed, and the doppler spectrum (or values derived from it) are recorded. Another sequence is then input and the cycle is repeated, etc., until all the data have been processed. Now examine one of these cycles; i.e., a sequence of discrete time-series values is in core memory as follows:

$$CH1(n) = CH1(n\Delta t), \quad n = 0, 1, 2, \ldots, N-1$$

$$CH2(n) = CH2(n\Delta t), \quad n = 0, 1, 2, \ldots, N-1$$

Where N = number of data samples being used in the calculations.

This data collection represents a time sequence selected at a random starting point as shown for one of the Doppler components:

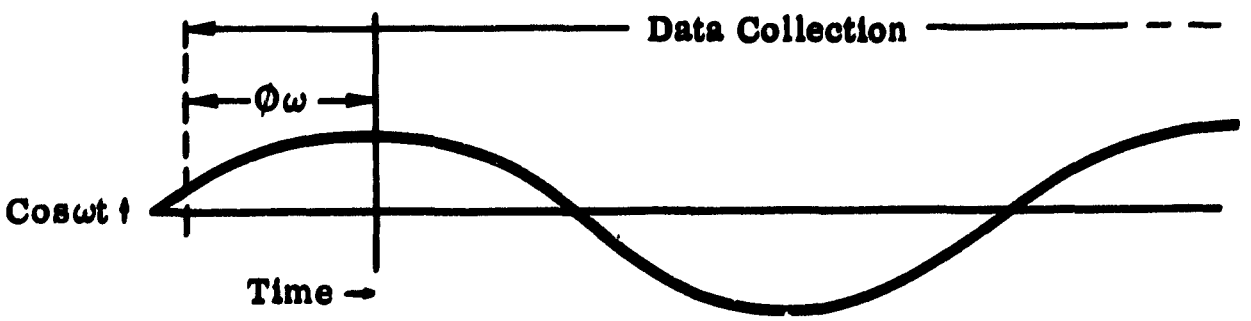

For any doppler component present in the signal, there will be a phase difference ϕ_ω of the component with respect to the beginning of the data sequence. Since the Fourier Transforms will preserve phase information relative to the beginning of the sequence, the two channels should be represented with respect to the starting point also:

$$CH1(n) = \frac{1}{2}(A_+ + A_-) \cos(\omega n\Delta t - \phi_\omega) \quad n = 0, 1, 2, \ldots, N-1$$

$$CH2(n) = \frac{1}{2}(A_+ - A_-) \sin(\omega n\Delta t - \phi_\omega)$$

Some useful relationships will now be developed; showing what happens to one component ω:

Let $x_1(n) = CH1(n) . \cos(\omega_0 n\Delta t)$

$$= \frac{1}{4}(A_+ + A_-)\cos[(\omega_0 + \omega)n\Delta t - \phi] + \frac{1}{4}(A_+ + A_-) \cos[(\omega_0 - \omega)n\Delta t + \phi_\omega]$$

[Identity used: $\cos x \cos y = \frac{1}{2}\cos(x+y) + \frac{1}{2}\cos(x-y)$]

$x_2(n) = CH2(n).\sin(\omega_0 n\Delta t)$

$$= \frac{1}{4}(A_- - A_+) \cos[(\omega_0 + \omega)n\Delta t - \phi_\omega)] + \frac{1}{4}(A_+ - A_-) \cos[(\omega_0 - \omega)n\Delta t + \phi_\omega)]$$

[Identity used: $\sin x \sin y = -\frac{1}{2}\cos(x+y) + \frac{1}{2}\cos(x-y)$]

Now form

$$x_3(n) = x_1(n) + x_2(n) = \tfrac{1}{2}A_- \cos[(\omega_0 + \omega)n\Delta t - \phi_\omega]$$

$$+ \tfrac{1}{2}A_+ \cos[(\omega_0 - \omega)n\Delta t + \phi_\omega)]$$

$$x_4(n) = x_1(n) - x_2(n) = \tfrac{1}{2}A_+ \cos[(\omega_0 + \omega)n\Delta t - \phi_\omega)]$$

$$+ \tfrac{1}{2}A_- \cos[(\omega_0 - \omega)n\Delta t + \phi_\omega]$$

Now for $\omega_0 = \omega$,

$$x_3(n) = \tfrac{1}{2}A_- \cos[(2\omega)n\Delta t - \phi_\omega] + \tfrac{1}{2}A_+ \cos\phi_\omega$$

$$x_4(n) = \tfrac{1}{2}A_+ \cos[(2\omega)n\Delta t - \phi_\omega] + \tfrac{1}{2}A_- \cos\phi_\omega$$

The 2ω terms here exceed the sampling resolution, but their amplitudes will be harmlessly folded to some other frequency. The useful property of x_3 and x_4 is that they have D.C., or "average" values equal to $\frac{1}{2}A_+ \cos\phi_\omega$ and $\frac{1}{2}A_- \cos\phi_\omega$, respectively; i.e.,

$$\tfrac{1}{2}A_+(\omega)\cos\phi_\omega(\text{average}) = \frac{1}{N}\sum_{n=0}^{N-1} x_3(n)$$

$$\tfrac{1}{2}A_-(\omega)\cos\phi_\omega(\text{average}) = \frac{1}{N}\sum_{n=0}^{N-1} x_4(n)$$

But since $x_3(n) = x_1(n) + x_2(n)$, we can write

$$\frac{1}{2}A_+(\omega)\cos\phi_\omega = x_5(\omega) = \frac{1}{N}\sum_{n=0}^{N-1} CH1(n).\cos(\omega\, n\Delta t) + \frac{1}{N}\sum_{n=0}^{N-1} CH2\ (n)$$

$$\sin(\omega\, n\Delta t)$$

$$= \mathrm{Re}[\mathcal{F}_\omega(CH2)] \quad - \mathrm{Im}[\mathcal{F}_\omega(CH1)]$$

And since $x_4(n) = x_1(n) - x_2(n)$, we can write

$$A_-(\omega)\cos\phi_\omega = x_6(\omega) = \mathrm{Re}[\mathcal{F}_\omega\ (CH1)] + \mathrm{Im}[\mathcal{F}_\omega(CH2)]$$

We then have the amplitudes $A_+(\omega)$ and $A_-(\omega)$ for any doppler frequency ω, except for the $\cos\phi_\omega$ factor.

Now examine what happens if we reverse the role of CH1 and CH2 and repeat the preceding logic:

Let

$$\hat{x}_1(n) = CH2(n).\cos(\omega_0 n\Delta t)$$

$$= \frac{1}{2}(A_+ - A_-)\sin(\omega n\Delta t - \phi).\cos(\omega_0 n\Delta t)$$

$$\hat{x}_2(n) = CH1(n).\sin(\omega_0 n\Delta t)$$

$$= \frac{1}{2}(A_+ + A_-)\cos(\omega n\Delta t - \phi).\sin(\omega_0 n\Delta t)$$

Form

$$\hat{x}_3(n) = \hat{x}_1(n) + \hat{x}_2(n)$$

$$= \frac{1}{2}(A_+ - A_-)\sin(\omega n\Delta t \cdot \phi_\omega)\cos(\omega_0 n\Delta t) + \frac{1}{2}(A_+ + A_-)$$

$$\cos(\omega n\Delta t - \phi_\omega)\sin(\omega_0 n\Delta t)$$

$$= \tfrac{1}{2}A_+ \sin[(\omega_0 + \omega)n\Delta t - \phi_\omega] + \tfrac{1}{2}A_- \sin[(\omega_0 - \omega)n\Delta t + \phi_\omega]$$

Similarly,

$$\hat{x}_4(n) = \hat{x}_1(n) - \hat{x}_2(n)$$

$$= \tfrac{1}{2}A_- \sin[(\omega_0 + \omega)n\Delta t - \phi] - \tfrac{1}{2}A_+ \sin[(\omega_0 - \omega)n\Delta t + \phi_\omega]$$

Once again, for $\omega_0 = \omega$, we get a dc component;

$$\hat{x}_5(n) = \hat{x}_3(n) \text{ (average)} = \tfrac{1}{2}A_- \sin\phi_\omega = -\mathrm{Im}[\mathcal{F}_\omega(\mathrm{CH1})] + \mathrm{Re}[\mathcal{F}_\omega(\mathrm{CH2})]$$

$$\hat{x}_6(n) = \hat{x}_4(n) \text{ (average)} = \tfrac{1}{2}A_+ \sin\phi_\omega = \mathrm{Im}[\mathcal{F}_\omega(\mathrm{CH1})] + \mathrm{Re}[\mathcal{F}_\omega(\mathrm{CH2})]$$

We again have the desired quantities $A_+(\omega)$ and $A_-(\omega)$, except this time there is an unwanted $\sin\phi_\omega$ term.

Now form

$$x_7(\omega_0) = [x_5(\omega)]^2 + [x_6(\omega)]^2$$

$$= [\tfrac{1}{2}A_+(\omega)\cos\phi_\omega]^2 + [\tfrac{1}{2}A_+(\omega)\sin\phi_\omega]^2$$

$$= \tfrac{1}{4}A_+^2(\omega)\cos^2\phi_\omega + \tfrac{1}{4}A_+^2(\omega)\sin^2\phi_\omega$$

$$= \tfrac{1}{4}A_+^2(\omega)(\cos^2\phi_\omega + \sin^2\phi_\omega)$$

$$= \tfrac{1}{4}A_+^2(\omega)$$

And likewise form

$$x_8(\omega_0) = [x_6(\omega)]^2 + [x_5(\omega)]^2$$

$$= \frac{1}{4}A_-^2(\omega_0)$$

Note that the phase angle ϕ_ω drops out and the $A_+(\omega)$ and $A_-(\omega)$ amplitudes for any frequency ω can be derived from x_5, x_6, $\hat{x}_5$, and $\hat{x}_6$, which are simple combinations of the Fourier Transforms of CH1 and CH2. A summary of the procedure follows:

Step 1. Input N values of CH1 and N values of CH2.

Step 2. Compute the Fast Fourier Transform of CH1, $\mathcal{F}$(CH1), and also $\mathcal{F}$(CH2). The result will be $\frac{N}{2}$ complex values for each transform:

$$\mathcal{F}_\omega(CH1) = Re[\mathcal{F}_\omega(CH1) - j\ Im[\mathcal{F}_\omega(CH1)]; \qquad j = \sqrt{-1}$$

$$\mathcal{F}_\omega(CH2) = Re[\mathcal{F}\omega(CH2) - j\ Im[\mathcal{F}_\omega(CH2)]$$

The $\mathcal{F}_\omega$ will be computed at the frequencies

$$\omega = 0, \omega_1, 2\omega_1, 3\omega_1, \ldots, (\frac{N}{2} - 1)\omega_1$$

Where $\omega_1 = 2\pi(n\Delta t)$

Step 3. For the doppler frequencies of interest, compute the positive and negative squared amplitudes by

$$\frac{1}{4}A_+^2(\omega) = \{Re[\mathcal{F}_\omega(CH1)] - Im[\mathcal{F}_\omega(CH2)]\}^2 + \{Im[\mathcal{F}_\omega(CH1)] + Re[\mathcal{F}_\omega(CH2)]\}^2$$

$$\frac{1}{4}A_{-}^{2}(\omega) = \{Re[\mathcal{F}_{\omega}(CH1)] + Im[\mathcal{F}_{\omega}(CH2)]\}^{2} + \{-Im[\mathcal{F}_{\omega}(CH1)] + Re[\mathcal{F}_{\omega}(CH2)]\}^{2}$$

The squared amplitudes may then be summed over frequency bands of interest to simulate bandpass filtering.

Note: In the MSC computer program, the Fourier coefficients are smoothed by "Hanning."

GLOSSARY OF TERMS

CH1(n) = The digitized, scaled time sequence representing the "in-phase" channel; i.e., this channel leads the second channel by 90° at all frequencies.

CH2(n) = The digitized, scaled time sequence representing the "out-of-phase" channel; i.e., this channel lags the first channel by 90°.

$\mathcal{F}(\xi)$ = The Fast Fourier Transform of ξ

$\mathcal{F}_\omega(\xi)$ = The Fourier coefficient from the transform of the function ξ corresponding to the particular angular frequency ω.

$Re[\mathcal{F}_\omega(\xi)]$ = Real part of $\mathcal{F}_\omega(\xi)$

Im (ξ) = Imaginary part of $\mathcal{F}_\omega(\xi)$

$A_+(\omega)$ = Positive doppler amplitude at angular frequency ω (Fore Beam)

$A_-(\omega)$ = Negative doppler amplitude at angular frequency ω (Aft Beam)

ϕ_ω = Phase of the component with angular frequency ω, with respect to beginning of integration interval.

APPENDIX B

DATA VALIDATION PROGRAM

A computer subroutine is required to identify invalid data and halt the processing when performed on useless data. This subroutine will use the PSD curve and therefore should be inserted in FILTER portion of the program just behind the Fast Fourier Transform.

Data editing is accomplished by fitting a curve to segments of the data in turn. Data points which lie too far from the curve are replaced with computed points lying on the curve. Interference with the scatterometer reception by extraneous frequencies can be detected by data editing and a decision whether to correct for the interference or stop the present batch-processing can be made by computer, with suitable diagnostic printouts provided.

This appendix develops the algorithms required for data smoothing and determines the criteria for deciding upon the validity of data points.

The implementing of least-squares polynominal curve-fitting to given data can always be expressed as weighted sums of the data. These weights which are a function of the number of points to be considered in one application, and of the interval between points, are computed only once, and then always used. Data with Gaussian noise is smoothed and compressed by forming a weighted sum of measurements over a span of points and replacing the actual value at the midpoint by the weighted sum. Thus the smoothed value, y_o, at the midpoint of the twenty-one points

$$Y_{-10}, Y_{-9}, \ldots + Y_{-1}, Y_0, Y_1, Y_1, \ldots, Y_9, Y_{10}$$

is formed with the equation

$$Y_0 = W_{-10} Y_{-10} + W_{-9} Y_{-9} + \ldots + W_{-1} Y_{-1}$$

$$W_0 Y_0 + W, Y, + \ldots + W_9 Y_9 + W_{10} Y_{10} \qquad (1)$$

where the W_i have been pre-computed and stored in computer memory.

To evaluate the weights, W_i, the degree of polynominal and the number of measurements in the smoothing process must be determined. The PSD curve for scatterometer data can be assumed to be represented by the quadratic model

$$y = a + bx + cx^2 \qquad (2)$$

over spans of up to 80 adjacent data points. Here x is the frequency in Hz and y is the number of relative volts in decibels. The values of y are given at equal intervals of x (denoted Δx) which is a function of sampling rate. For example, Δx equals 12.20703 Hz for the 13.3 GHz vertically polarized scatterometer.

If the origin of coordinates is translated to the center point of n data points (n an odd number) the least-squares solution for a, b and c in (2) can be determined by the following arithmetical operations:

1. Form A and B:

$$A = \frac{\Delta x^2}{3} \quad p(p+1)\ (2p+1)$$

$$B = 2\Delta x^2\ (1^4 + 2^4 + \ldots + p^4)$$

where

$$p + 1/2(n-1) \qquad (3)$$

2. Form V_a, V_b, V_c, and V_{ac}:

$$V_a = \frac{B}{nB-A^2}$$

$$V_b = 1/A$$

$$V_c = \frac{n}{nB-A^2}$$

$$V_{ac} = \frac{-A}{nB-A^2}$$

3. Form Y_1, Y_2 and Y_3:

$$Y_1 = y_{-p} + y_{-p+1} + \ldots + y_{-1} + y_o + y_1 + \ldots + y_{p-1} + y_p \tag{4}$$

$$Y_2 = \Delta x \left[-py_{-p} - (p-1)\, y_{-p+1} - \ldots - y_{-1} + y_1 + \ldots + (p-1)y_{p-1} + py_p \right] \tag{5}$$

$$Y_3 = \Delta x^2 \left[p^2 y_{-p} + (p-1)^2 y_{-p+1} + \ldots + y_{-1} + y_1 + \ldots + (p-1)^2 y_{p-1} + p^2 y_p \right] \tag{6}$$

The least squares solution for a, b and c are then given by three equations:

$$a = V_a Y_1 + V_{ac} Y_3 \tag{7}$$

$$b = V_b Y_2 \tag{8}$$

$$c = V_{ac} Y_1 + V_c Y_3 \tag{9}$$

For $x = 0$, that is, the midpoint, the best estimate for y is

$$\hat{y}_o = a \tag{10}$$

by the least-squares criterion, and to compute adjusted data points the equation

$$\hat{y}_i = a + bi\Delta x + ci\Delta x^2 \tag{11}$$

$(i = -p, -p+1, \ldots, -1, 0, 1, \ldots, p-1, p)$

is utilized.

To program (7), (8) and (9) in a form for most efficient computation, a, b and c are all written as weighted sums of the data:

$$a = u_{-p}\,y_{-p} + u_{-p+1}\,y_{-p+1} + \ldots + u_{-1}y_{-1}$$

$$+u_o y_o + u_1 y_1 + \ldots + u_{p-1}y_{p-1} + u_p y_p \qquad (12)$$

$$b = v_{-p}y_{-p} + v_{-p+1}y_{-p+1} + \ldots + v_{-1}y_{-1}$$

$$+v_o y_o + v, y, + \ldots + v_{p-1}y_{p-1} + v_p y_p \qquad (13)$$

$$c = w_{-p}y_{-p} + w_{-p+1}y_{-p+1} + \ldots + w_{-1}y_{-1}$$

$$+w_o y_o + w_1 y_1 + \ldots + w_{p-1}y_{p-1} + w_p y_p \qquad (14)$$

where the u, v and w arrays are derived by substituting (4), (5) and (6) into (7), (8) and (9). Performing this substitution, it is found that

$$u_i = u_{-i}$$

$$v_i = v_{-1}$$

$$w_i = w_{-i}$$

$$(i = 1, 2, \ldots, p)$$

and the p+1 equations for the weights may be written as follows:

$$u_o = V_a \qquad w_o = 0$$

$$u_1 = V_a + V_{ac}\Delta x^2 \qquad w_1 = V_{ac} + V_c\,\Delta x^2$$

$$u_2 = V_a + 4V_{ac}\Delta x^2 \qquad w_2 = V_{ac} + 4V_c\,\Delta x^2$$

$$\vdots \qquad\qquad \vdots$$

$$u_{p-1} = V_a + V_{ac}(p-1)^2\,\Delta x^2 \qquad w_{p-1} = V_{ac} + (p-1)^2\,V_c\,\Delta x^2$$

$$u_p = V_a + V_{ac}\,p^2\,\Delta x^2 \qquad w_p = V_{ac} + p^2 V_c\,\Delta x^2$$

$$v_o = 0$$

$$v_1 = V_b\,\Delta x$$

$$v_2 = 2V_b\,\Delta x$$

$$\vdots$$

$$v_{p-1} = (p-1)V_b\,\Delta x$$

$$v_p = pV_b\,\Delta x$$

The variance of the adjusted value of the midpoint, σ_y^2, can be computed with

$$\sigma_{\hat{y}}^2 = \frac{B}{nB-A^2}\,\sigma_y^2 \qquad (15)$$

where σ_y is the rms of the differences between pairs of raw data values and data values computed using (11). The square root of the variance, the standard deviation, is a measure of the validity of the data and is the criterion by which data is edited and justified for validity.

The deviation of a data point from the least-squares curve point corresponding, will have a probability of 68.3% of being less than $1\sigma_{\hat{y}}$, 95.4% of being less than $2\sigma_{\hat{y}}$ and 99.7% of being less than $3\sigma_{\hat{y}}$. Thus, on the average, only three points out of a thousand should scatter from the least-squares value by more than $3\sigma_{\hat{y}}$, and if significantly more than three points do diverge farther than $3\sigma_{\hat{y}}$, it is an indication that data on this part of the PSD curve is invalid. Exactly what multiple of $\sigma_{\hat{y}}$ will be employed for the criterion will be established by trial and error, with an initial value of $3\sigma_{\hat{y}}$.

Invalid data will be tested to determine whether its frequency lies within one of the bandwidths defining the angles of the σ_o curve, and if so, that point of the σ_o curve will not be computed, for it would be erroneous.

To summarize, the data validation computer subroutine will perform the following steps:

1. With the first n points of the PSD curve, form a, b, and c with (12, (13), and (14), using the pre-computed weights. (The value of n must be determined by experimenting with data. Initial trial values will be 21, 31, and 41).

2. For $3\sigma_y$ employing (11) and (15).

3. Test the n differences, data points minus computed points, to identify points deviating by more than $3\sigma_{\hat{y}}$.

4. Test the frequencies of "wild" points to determine whether they lie in an angle-defining bandwidth. If so, do not form σ_o for that angle.

5. Do steps 1 to 4 with the next n points and continue until all points are processed.

APPENDIX C

CHARACTERISTIC PROBLEMS IDENTIFIED THROUGH DATA VALIDATION PROCEDURES

This appendix contains actual analog and digital outputs Figures C-1 to C-12. Each is an example of one or more of the system, collection, and reduction problems outlined earlier in Table 5-1.

Table 5-1 is repeated here for convenience in referring to the various error categories. Also included on each figure is a summarizing statement on the means of extracting as much useful data as possible from such line.

TABLE 5-1

PROBLEM CATEGORIES	CONTRIBUTING FACTORS PREVIOUSLY ISOLATED	VARIATION NOTED IN DATA (SEE APPENDIX A FOR EXAMPLES)
(1) 60 Hz Interference (When system operated on 60 Hz power)	60 Hz power supply ripple	Large spike at 60 Hz noted in PSD spikes of 60 Hz harmonics at other frequencies
(2) 400 Hz Interference	(a) Inadequate cable shielding and other wiring problems	(a) Large spike at 400 Hz on PSD spikes of 400 Hz harmonics at other frequencies
	(b) Inadequate aircraft ground connections	(b) Poor overall dynamic range noted in both PSD and time histories.
	(c) Faulty patch panel connections	
	(d) 400 Hz power supply ripple	
(3) excessively high noise level	(a) Bad crystal diode	(a) Poor dynamic range on PSD's and time histories. Range measured from highest signal to noise floor less than 20 db.
	(b) Improper equipment operation during data playback procedure	(b) db level at 9 KHz is higher than the level at a frequency less than 9 KHz on time history
	(c) Improper tape recorder operation during tape dubbing procedure	(c) 9 KHz noise floor follows signal at other frequencies on time histories.
	(d) Improper gain factor used in equipment during data collection causes tape recorder saturation onboard aircraft	

PROBLEM CATEGORIES	CONTRIBUTING FACTORS PREVIOUSLY ISOLATED	VARIATION NOTED IN DATA (SEE APPENDIX A FOR EXAMPLES)
(4) Poorly defined calibrate signal level	(a) Lack of accurate speed control on data playback recorder	(a) Ragged 10 KHz spike with rounded peak as plotted on PSD.
	(b) Shut down of onboard equipment in middle of data collector	(b) Drop out of cal signal; periodic spikes on the cal signal; no cal signal at all as plotted versus time on time history.
	(c) Loose connection to the audio oscillator onboard aircraft	(c) Excessive variations in the cal signal of more than ± 3db for long periods of time noted on time history.
	(d) Saturation onboard tape recorder due to gain setting in overland mode and data collected over water	
(5) Periodic noise spikes which occur through the data	RC-8 camera's intervolameter pulsing circuit being picked up through faulty patch panel connection	Spike 5 to 6 db in amplitude appear most strongly in 9 KHz noise floor as plotted on time history. These spikes occur through the data at intervals from 5 to 10 seconds long depending on aircraft altitude.

PROBLEM CATEGORIES	CONTRIBUTING FACTOR PREVIOUSLY ISOLATED	VARIATION NOTED IN DATA (SEE APPENDIX A FOR EXAMPLES)
(6) Oscillations and periodic interference	(a) Land based control radar tracking aircraft and being picked up on data channel	(a) Areas in data of few seconds duration which occurs in both channels as a periodic pattern. When viewed on oscilloscope these areas show sinusoidal characteristics with high millivolt levels.
	(b) Operation of equipment at extreme altitudes	(b) Periodic oscillations or interference patterns that are similar to those mentioned in (a) but occur in one channel only.
	(c) Poor transistor socket connections in equipment	(c) An interference pattern noted on PSD's at between 7 and 8 KHz. appears as a buildup in signal level which falls off beyond this point.
	(d) Possible propeller modulation being picked up at antenna	
	(e) Possible resonant frequency vibration of internal or external airframes section being picked up in data	

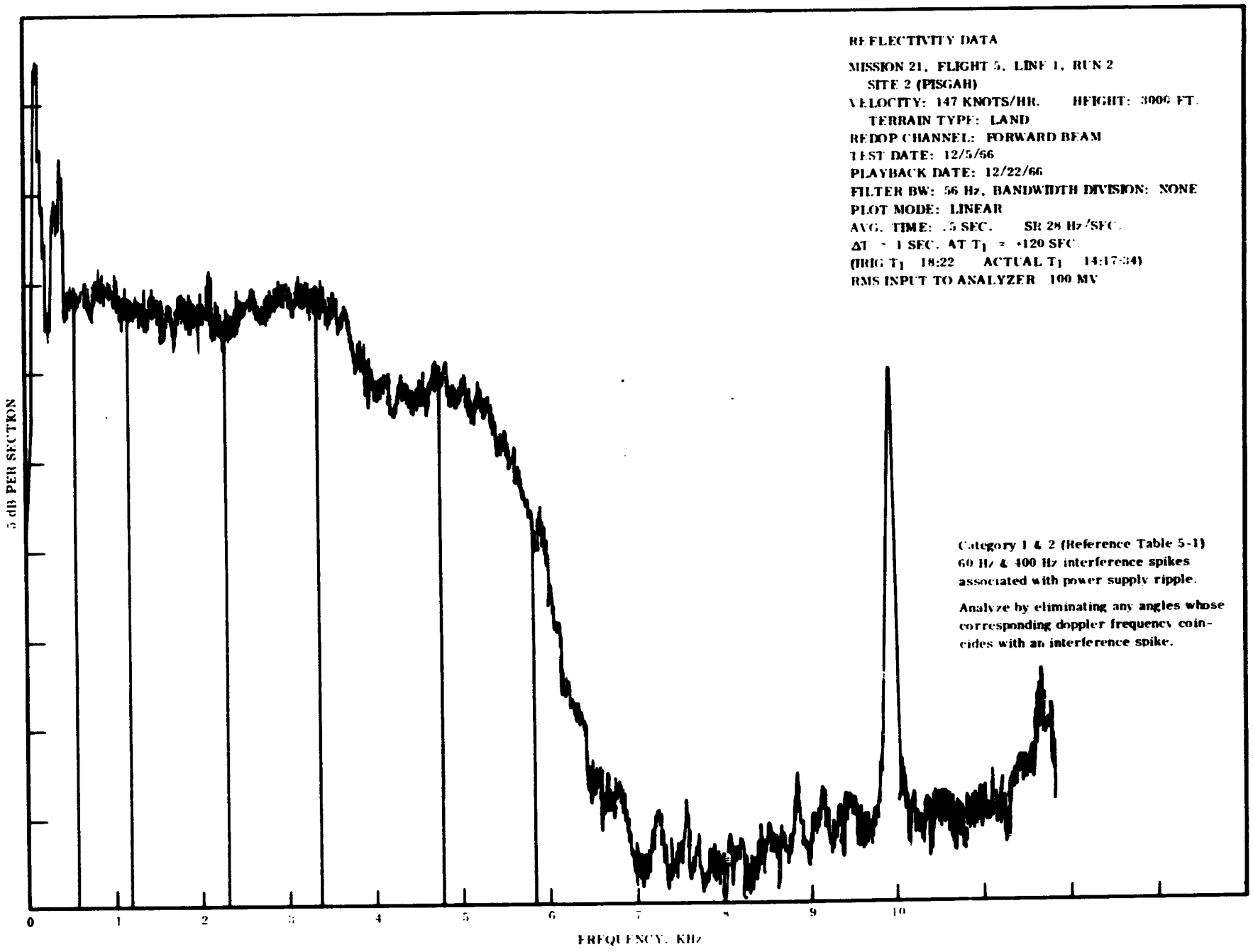
REFLECTIVITY DATA
MISSION 21, FLIGHT 5, LINE 1, RUN 2
SITE 2 (PISGAH)
VELOCITY: 147 KNOTS/HR. HEIGHT: 3006 FT.
TERRAIN TYPE: LAND
REDOP CHANNEL: FORWARD BEAM
TEST DATE: 12/5/66
PLAYBACK DATE: 12/22/66
FILTER BW: 56 Hz, BANDWIDTH DIVISION: NONE
PLOT MODE: LINEAR
AVG. TIME: .5 SEC. SR 28 Hz/SEC.
ΔT = 1 SEC. AT T1 = +120 SEC.
(IRIG T1 18:22 ACTUAL T1 14:17:34)
RMS INPUT TO ANALYZER 100 MV
5 dB PER SECTION
Category 1 & 2 (Reference Table 5-1)
60 Hz & 400 Hz interference spikes
associated with power supply ripple.
Analyze by eliminating any angles whose
corresponding doppler frequency coin-
cides with an interference spike.
0
1
2
3
4
5
6
7
8
9
10
FREQUENCY, KHz

Figure C-1

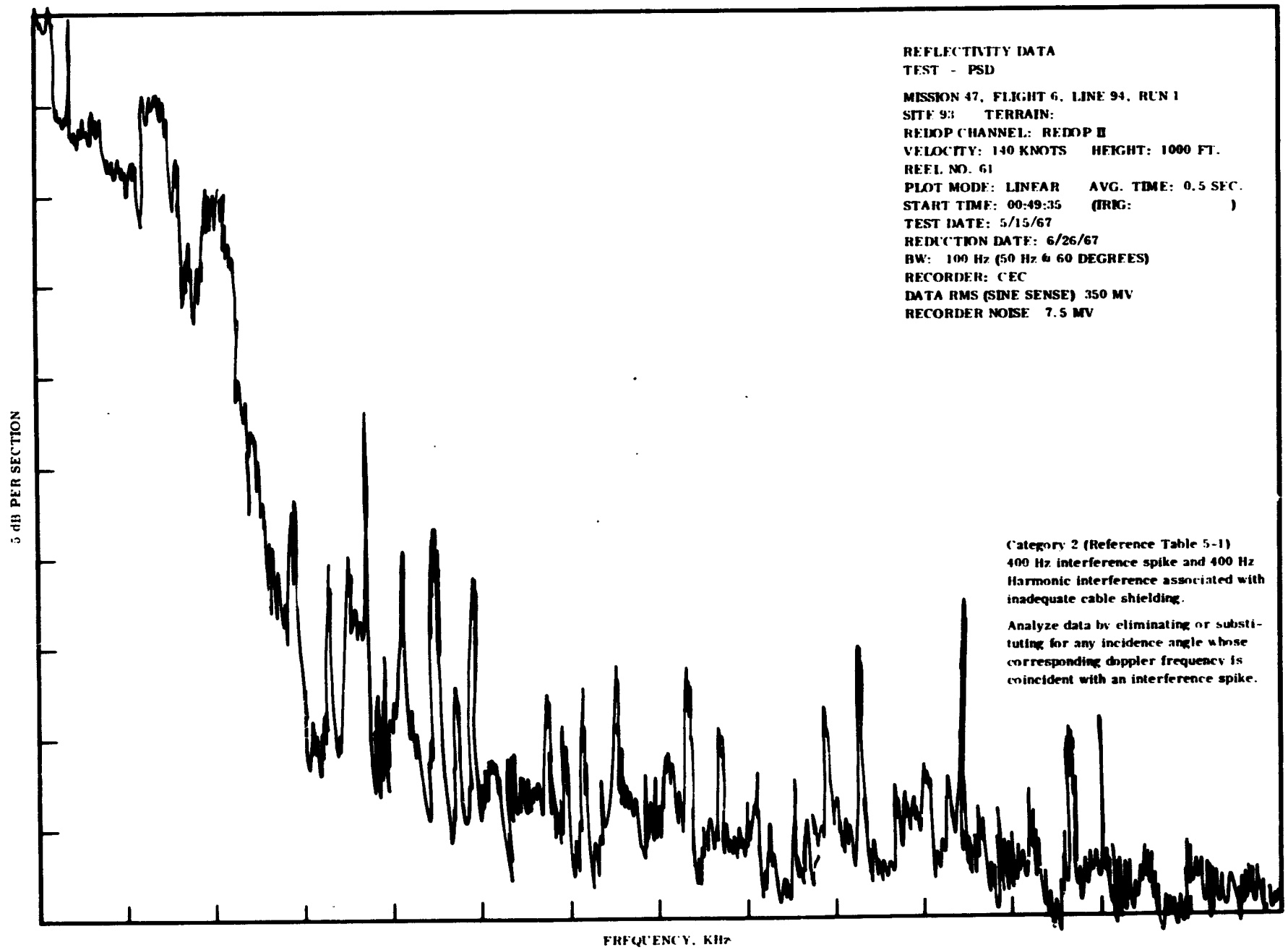
REFLECTIVITY DATA
TEST - PSD
MISSION 47, FLIGHT 6, LINE 94, RUN 1
SITE 93 TERRAIN:
REDOP CHANNEL: REDOP II
VELOCITY: 140 KNOTS HEIGHT: 1000 FT.
REEL NO. 61
PLOT MODE: LINEAR AVG. TIME: 0.5 SEC.
START TIME: 00:49:35 (IRIG:)
TEST DATE: 5/15/67
REDUCTION DATE: 6/26/67
BW: 100 Hz (50 Hz & 60 DEGREES)
RECORDER: CEC
DATA RMS (SINE SENSE) 350 MV
RECORDER NOISE 7.5 MV
5 dB PER SECTION
Category 2 (Reference Table 5-1)
400 Hz interference spike and 400 Hz Harmonic interference associated with inadequate cable shielding.
Analyze data by eliminating or substituting for any incidence angle whose corresponding doppler frequency is coincident with an interference spike.
FREQUENCY, KHz

Figure C-2

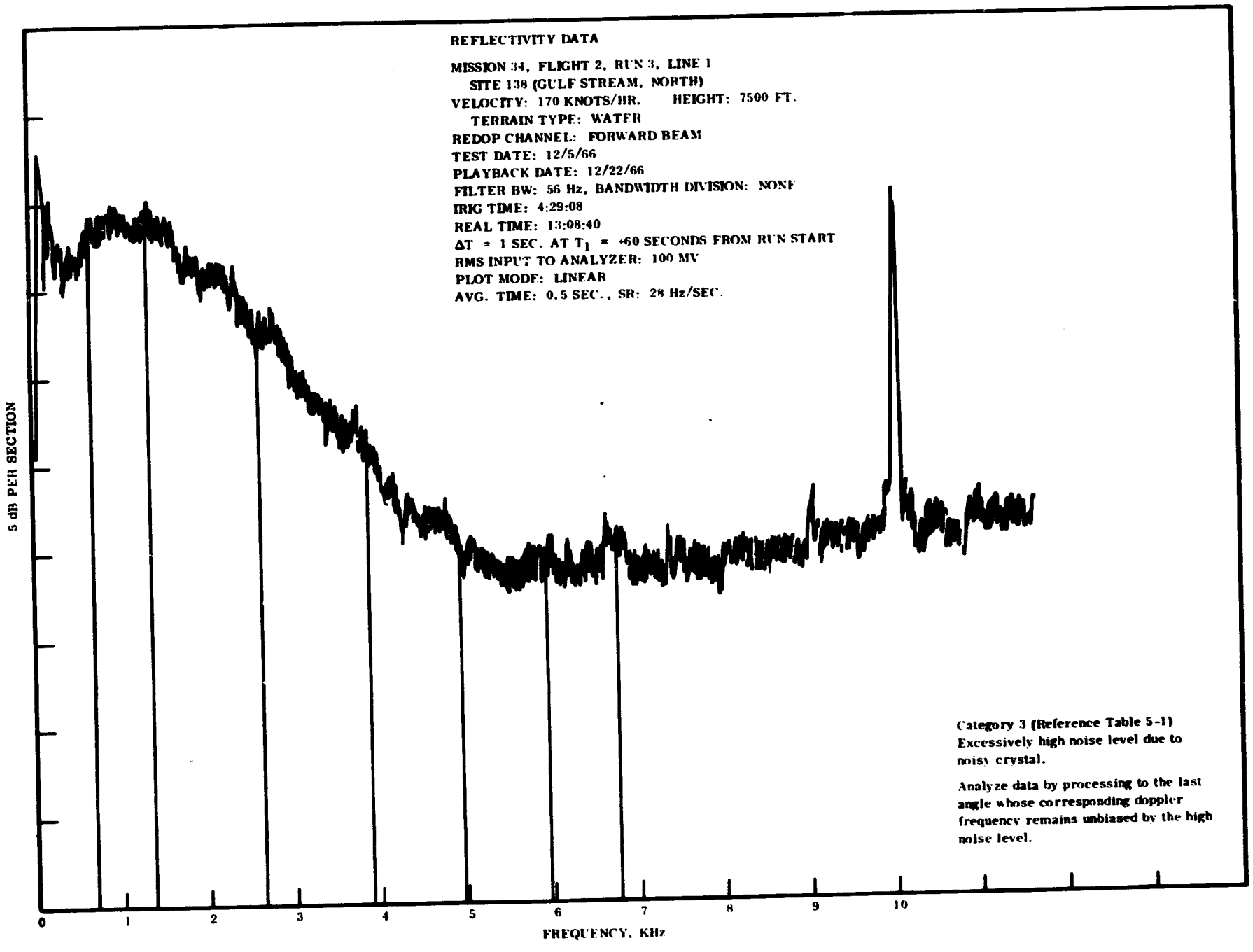
REFLECTIVITY DATA
MISSION 34, FLIGHT 2, RUN 3, LINE 1
SITE 138 (GULF STREAM, NORTH)
VELOCITY: 170 KNOTS/HR. HEIGHT: 7500 FT.
TERRAIN TYPE: WATER
REDOP CHANNEL: FORWARD BEAM
TEST DATE: 12/5/66
PLAYBACK DATE: 12/22/66
FILTER BW: 56 Hz, BANDWIDTH DIVISION: NONE
IRIG TIME: 4:29:08
REAL TIME: 13:08:40
ΔT = 1 SEC. AT T1 = +60 SECONDS FROM RUN START
RMS INPUT TO ANALYZER: 100 MV
PLOT MODE: LINEAR
AVG. TIME: 0.5 SEC., SR: 28 Hz/SEC.
5 dB PER SECTION
0
1
2
3
4
5
6
7
8
9
10
FREQUENCY, KHz
Category 3 (Reference Table 5-1)
Excessively high noise level due to noisy crystal.
Analyze data by processing to the last angle whose corresponding doppler frequency remains unbiased by the high noise level.

Figure C-3

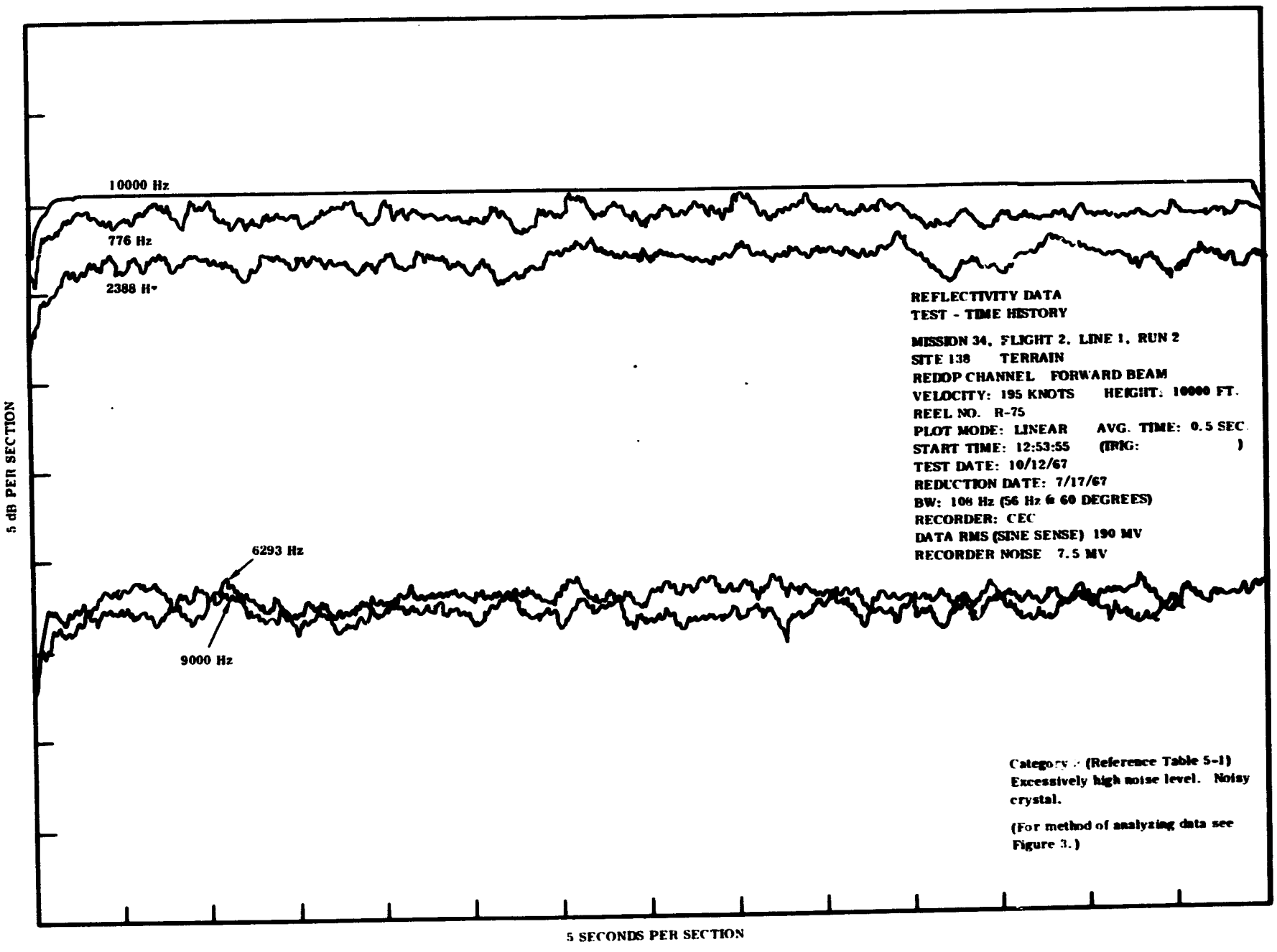
10000 Hz
776 Hz
2388 Hz
6293 Hz
9000 Hz
5 dB PER SECTION
5 SECONDS PER SECTION
REFLECTIVITY DATA
TEST - TIME HISTORY
MISSION 34, FLIGHT 2, LINE 1, RUN 2
SITE 138 TERRAIN
REDOP CHANNEL FORWARD BEAM
VELOCITY: 195 KNOTS HEIGHT: 10000 FT.
REEL NO. R-75
PLOT MODE: LINEAR AVG. TIME: 0.5 SEC.
START TIME: 12:53:55 (IRIG:)
TEST DATE: 10/12/67
REDUCTION DATE: 7/17/67
BW: 106 Hz (56 Hz @ 60 DEGREES)
RECORDER: CEC
DATA RMS (SINE SENSE) 190 MV
RECORDER NOISE 7.5 MV
Category 4 (Reference Table 5-1)
Excessively high noise level. Noisy crystal.
(For method of analyzing data see Figure 3.)

Figure C-4

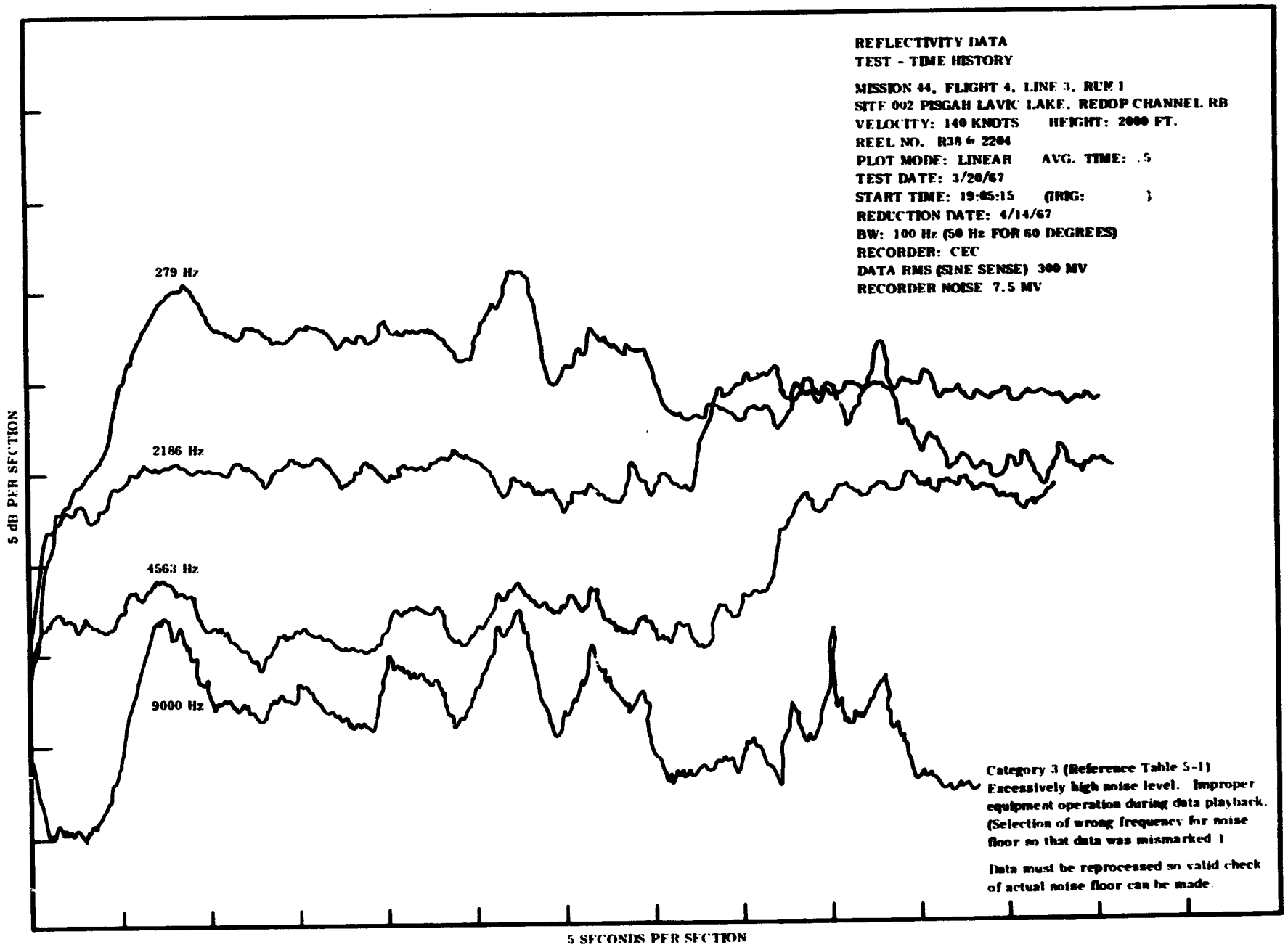
REFLECTIVITY DATA
TEST - TIME HISTORY
MISSION 44, FLIGHT 4, LINE 3, RUN 1
SITE 002 PISGAH LAVIC LAKE, REDOP CHANNEL RB
VELOCITY: 140 KNOTS HEIGHT: 2000 FT.
REEL NO. R38 & 2204
PLOT MODE: LINEAR AVG. TIME: .5
TEST DATE: 3/20/67
START TIME: 19:05:15 (IRIG:)
REDUCTION DATE: 4/14/67
BW: 100 Hz (50 Hz FOR 60 DEGREES)
RECORDER: CEC
DATA RMS (SINE SENSE) 300 MV
RECORDER NOISE 7.5 MV
279 Hz
2186 Hz
4563 Hz
9000 Hz
5 dB PER SECTION
5 SECONDS PER SECTION
Category 3 (Reference Table 5-1)
Excessively high noise level. Improper equipment operation during data playback. (Selection of wrong frequency for noise floor so that data was mismarked.)
Data must be reprocessed so valid check of actual noise floor can be made.

Figure C-5

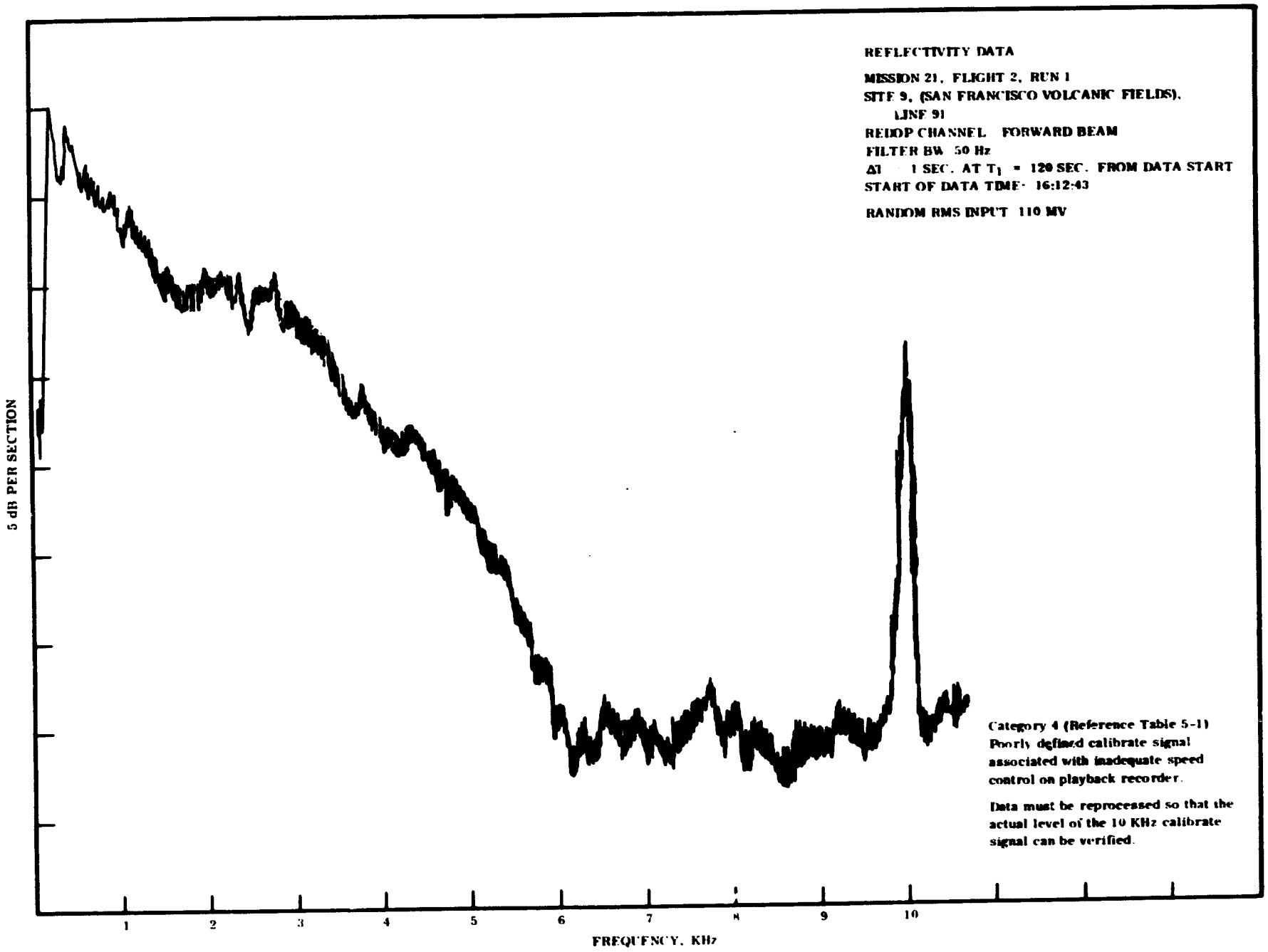
REFLECTIVITY DATA
MISSION 21, FLIGHT 2, RUN 1
SITE 9, (SAN FRANCISCO VOLCANIC FIELDS),
LINE 91
REDOP CHANNEL FORWARD BEAM
FILTER BW 50 Hz
Δt 1 SEC. AT T1 = 120 SEC. FROM DATA START
START OF DATA TIME- 16:12:43
RANDOM RMS INPUT 110 MV
5 dB PER SECTION
1
2
3
4
5
6
7
8
9
10
FREQUENCY, KHz
Category 4 (Reference Table 5-1)
Poorly defined calibrate signal
associated with inadequate speed
control on playback recorder.
Data must be reprocessed so that the
actual level of the 10 KHz calibrate
signal can be verified.

Figure C-6

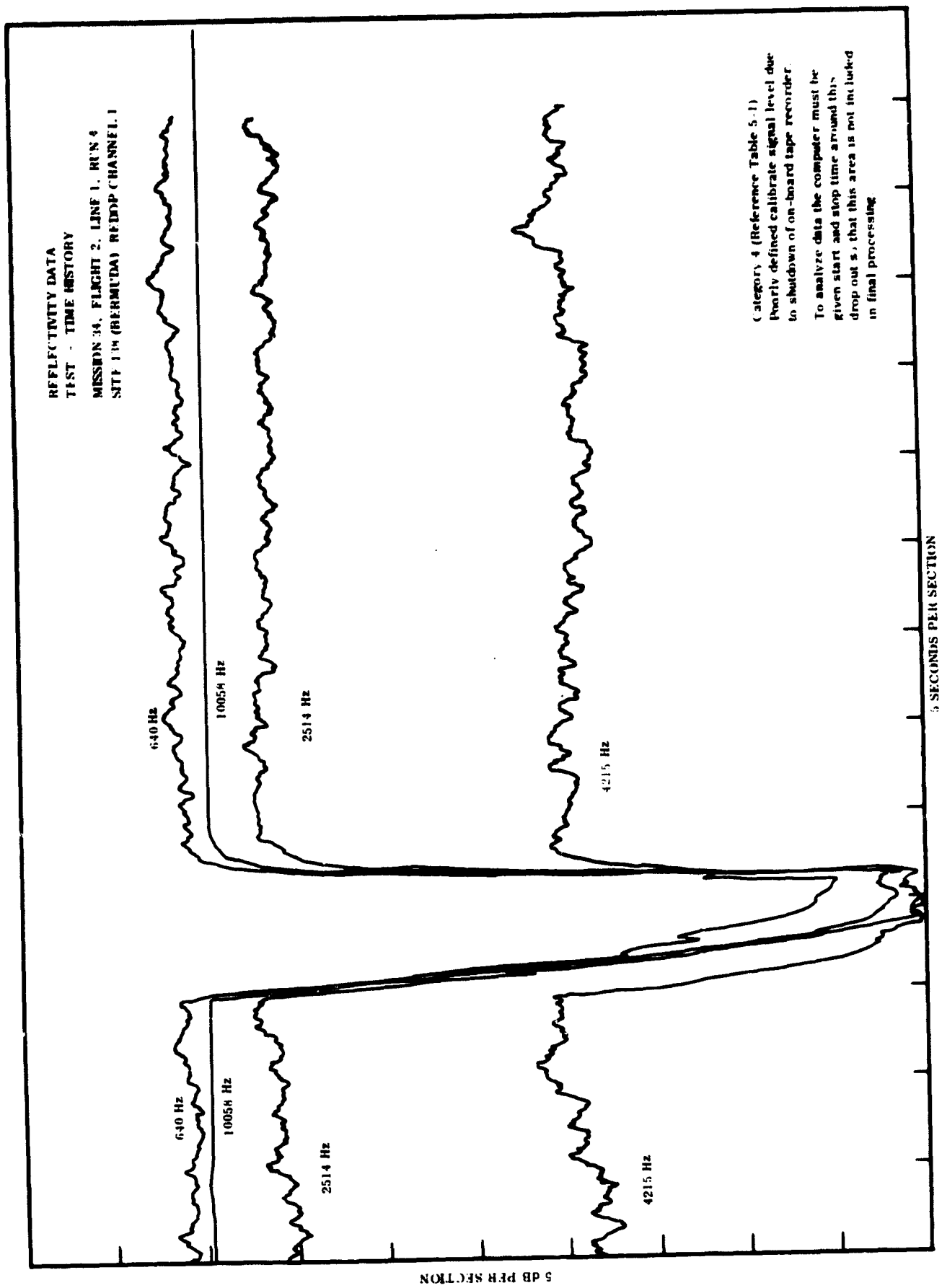
REFLECTIVITY DATA
TEST - TIME HISTORY
MISSION 38, FLIGHT 2, LINE 1, RUN 4
SITE 116 (BERMUDA) REDOP CHANNEL 1
640 Hz
1005.8 Hz
2514 Hz
4215 Hz
Category 4 (Reference Table 5-1)
Poorly defined calibrate signal level due to shutdown of on-board tape recorder
To analyze data the computer must be given start and stop time around this drop out s, that this area is not included in final processing
5 SECONDS PER SECTION
5 DB PER SECTION

Figure C-7

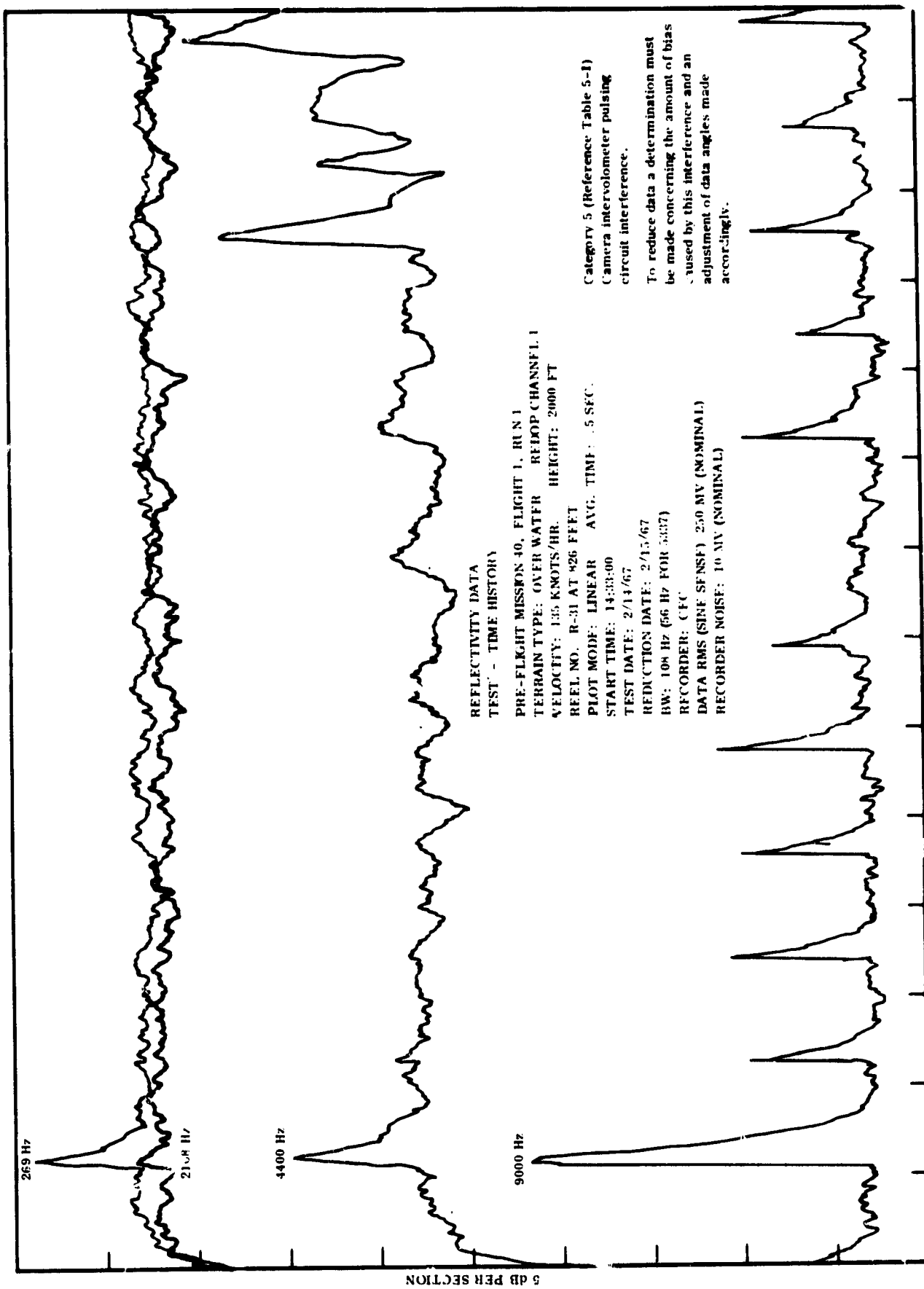
269 Hz
4400 Hz
9000 Hz
REFLECTIVITY DATA
TEST - TIME HISTORY
PRE-FLIGHT MISSION 40, FLIGHT 1, RUN 1
TERRAIN TYPE: OVER WATER REDOP CHANNEL 1
VELOCITY: 135 KNOTS/HR. HEIGHT: 2000 FT
REEL NO. R-31 AT 926 FEET
PLOT MODE: LINEAR AVG. TIME: .5 SEC.
START TIME: 14:38:00
TEST DATE: 2/14/67
REDUCTION DATE: 2/15/67
BW: 104 Hz (56 Hz FOR 5837)
RECORDER: CEC
DATA RMS (SINE SENSE) 250 MV (NOMINAL)
RECORDER NOISE: 10 MV (NOMINAL)
Category 5 (Reference Table 5-I)
Camera intervolometer pulsing
circuit interference.
To reduce data a determination must
be made concerning the amount of bias
caused by this interference and an
adjustment of data angles made
accordingly.
5 dB PER SECTION
TIME, 5 SECONDS PER SECTION

Figure C-8

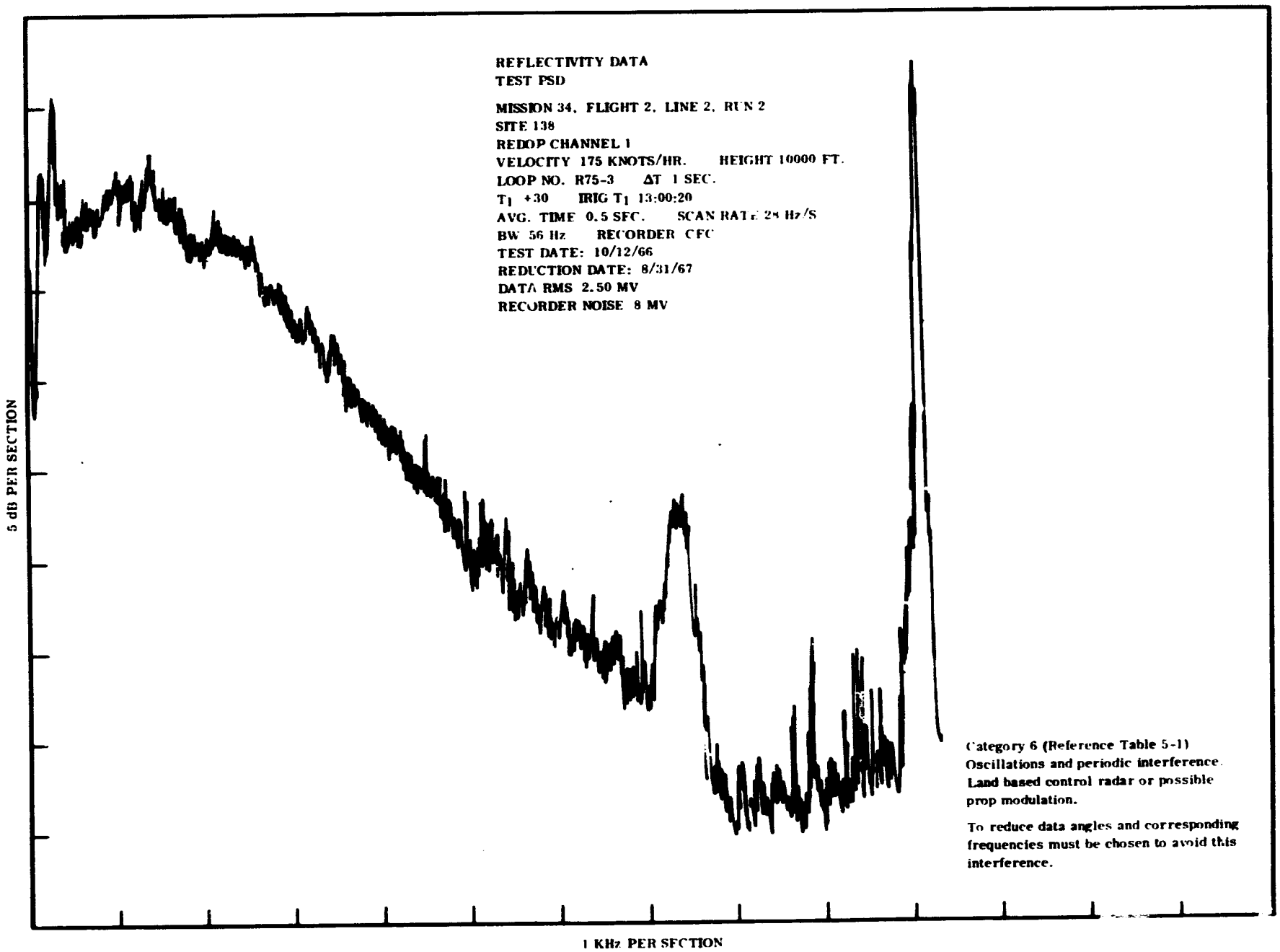
REFLECTIVITY DATA
TEST PSD
MISSION 34, FLIGHT 2, LINE 2, RUN 2
SITE 138
REDOP CHANNEL 1
VELOCITY 175 KNOTS/HR. HEIGHT 10000 FT.
LOOP NO. R75-3 ΔT 1 SEC.
T1 +30 IRIG T1 13:00:20
AVG. TIME 0.5 SEC. SCAN RATE 25 Hz/S
BW 56 Hz RECORDER CEC
TEST DATE: 10/12/66
REDUCTION DATE: 8/31/67
DATA RMS 2.50 MV
RECORDER NOISE 8 MV
5 dB PER SECTION
1 KHz PER SECTION
Category 6 (Reference Table 5-1)
Oscillations and periodic interference.
Land based control radar or possible
prop modulation.
To reduce data angles and corresponding
frequencies must be chosen to avoid this
interference.

Figure C-9

NOTE: Digital Check Procedures show erroneous data point (60 degrees) biased leg noise during digitizing. (New system has eliminated this problem.)

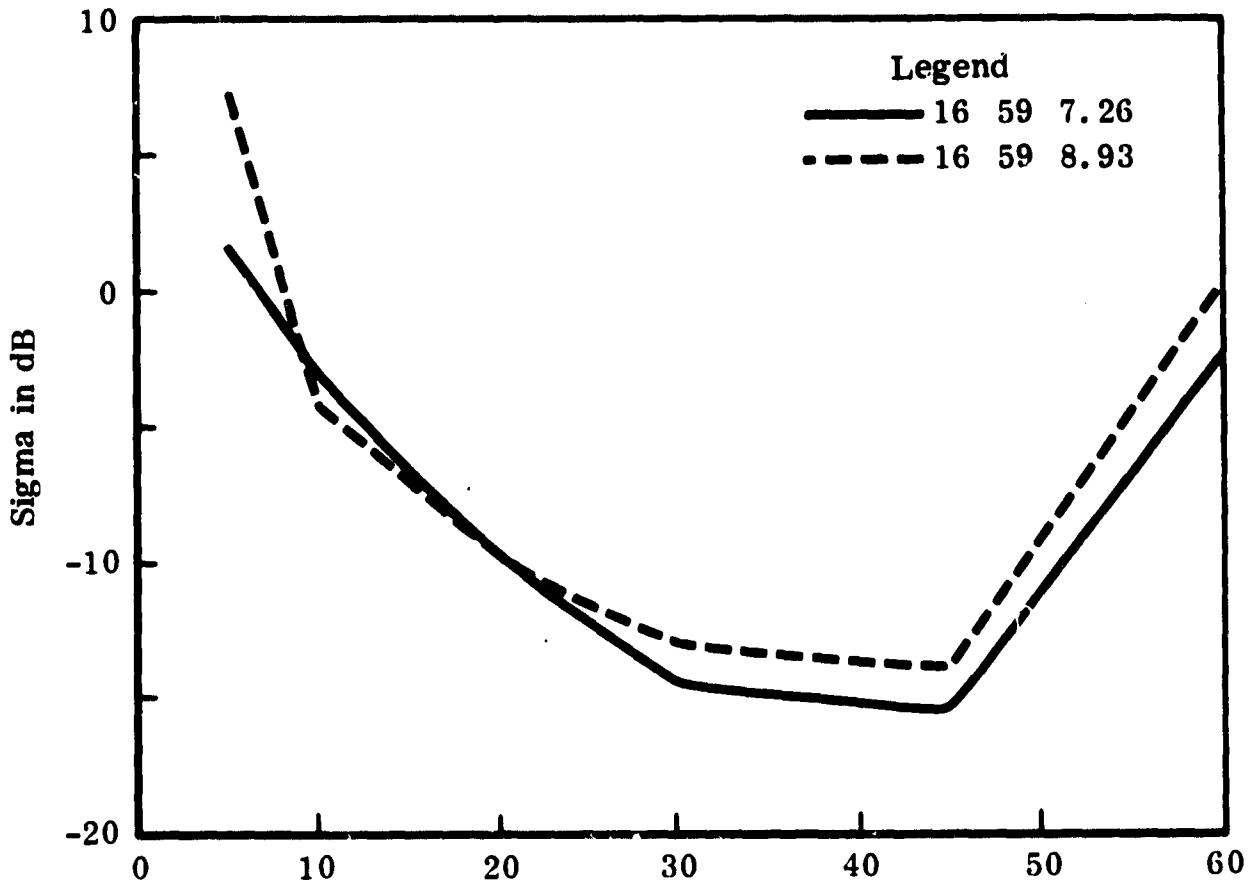

National Aeronautics and Space Administration
Manned Spacecraft Center - Houston
Scatterometer Mission 21
Flight 12 Line 1
Run 3 Site 10
Tapes 17628 17629 Fore Scatter

Figure C-10 Reflectivity Plot

NOTE: Digital Check Procedures show similar problem to that shown in Figure 10. However, the problem occurred in the downward direction and at a different incidence angle 20 degrees.

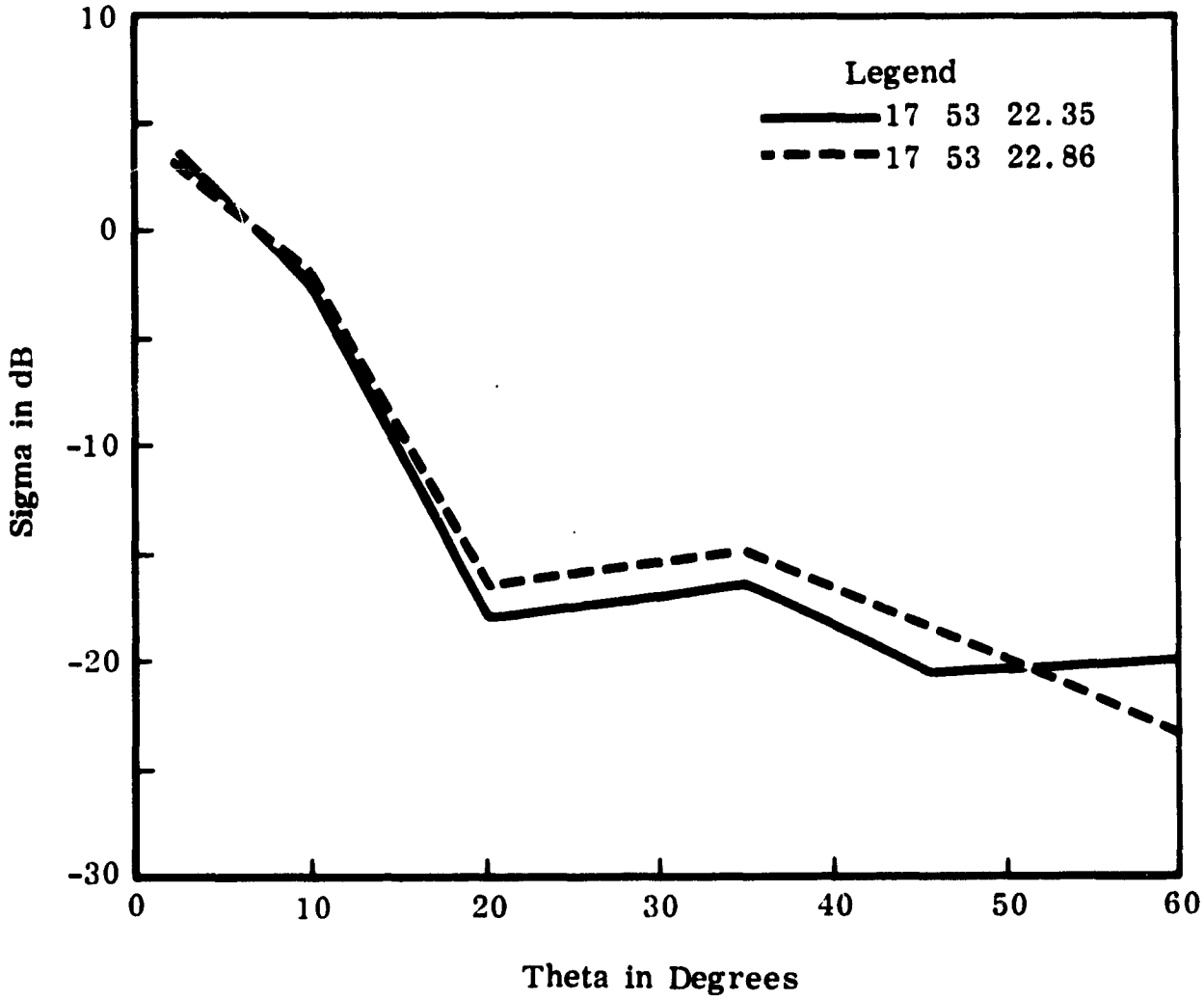

National Aeronautics and Space Administration
Manned Spacecraft Center - Houston
Scatterometer Mission 39
Flight 1 Line 93
Run 3 Site 114
Tapes 33499 33498 Aft Scatter

Figure C-11 Reflectivity Plot

NOTE: Digital Check Procedures show an error during processing through digital filtering program. Data is plotted at constant level for several seconds. (Tests have been run to identify and eliminate this problem.)

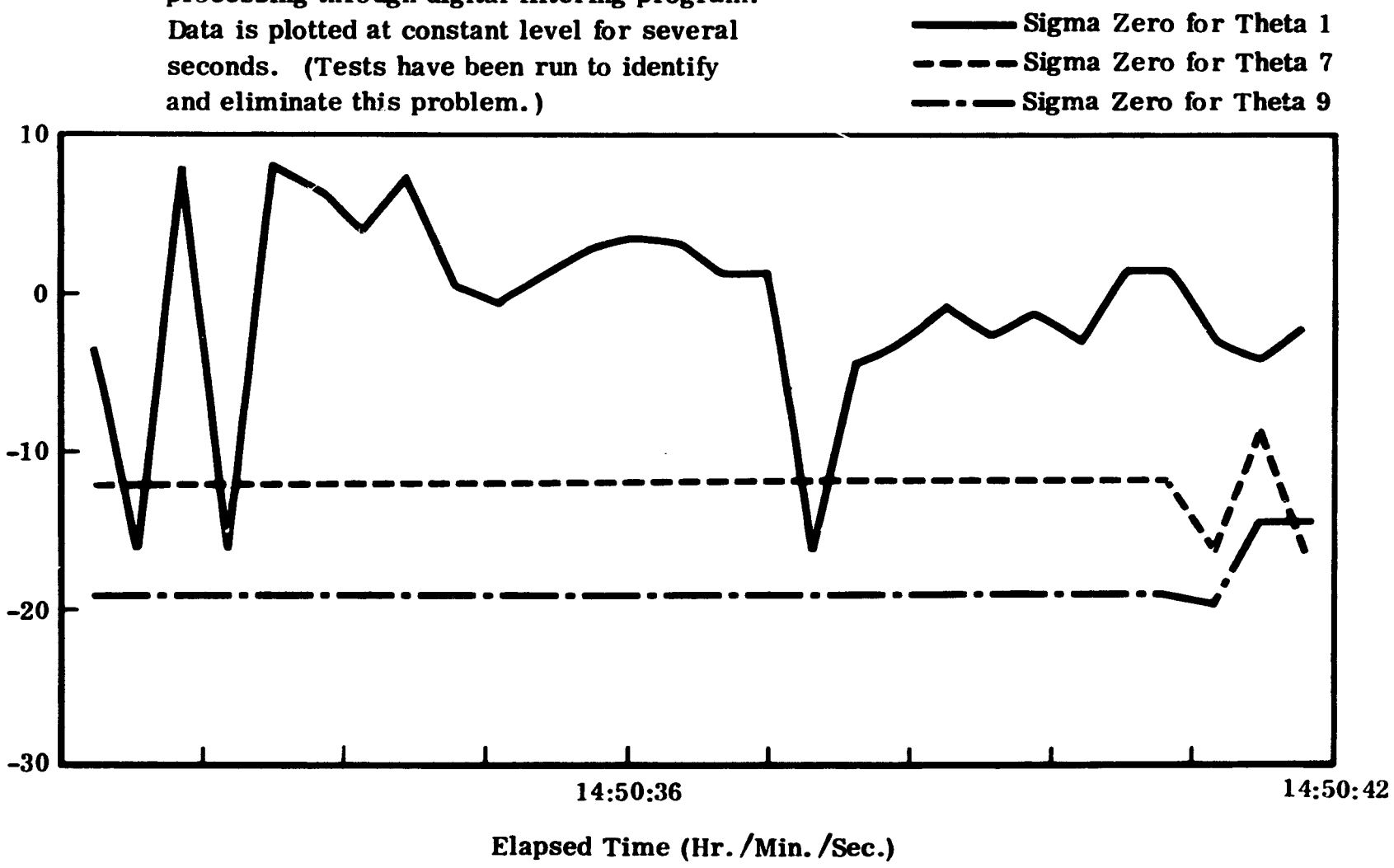

Figure C-12 Sigma Plots: Mission 77, Flight 2, Line 31, Run 1, Site 44, 871 AFT